



# The East Anatolia–Lesser Caucasus ophiolite: An exceptional case of large-scale obduction, synthesis of data and numerical modelling

Y Rolland, M Hässig, Delphine Bosch, O Bruguier, R Melis, G Galoyan, G Topuz, L Sahakyan, A Avagyan, M. Sosson

## ► To cite this version:

Y Rolland, M Hässig, Delphine Bosch, O Bruguier, R Melis, et al.. The East Anatolia–Lesser Caucasus ophiolite: An exceptional case of large-scale obduction, synthesis of data and numerical modelling. *Geoscience Frontiers*, 2020, 11 (1), pp.83-108. 10.1016/j.gsf.2018.12.009 . hal-03017194

HAL Id: hal-03017194

<https://hal.science/hal-03017194>

Submitted on 20 Nov 2020

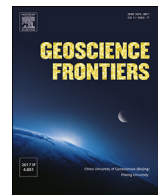
**HAL** is a multi-disciplinary open access archive for the deposit and dissemination of scientific research documents, whether they are published or not. The documents may come from teaching and research institutions in France or abroad, or from public or private research centers.

L'archive ouverte pluridisciplinaire **HAL**, est destinée au dépôt et à la diffusion de documents scientifiques de niveau recherche, publiés ou non, émanant des établissements d'enseignement et de recherche français ou étrangers, des laboratoires publics ou privés.



Contents lists available at ScienceDirect

China University of Geosciences (Beijing)

**Geoscience Frontiers**journal homepage: [www.elsevier.com/locate/gsf](http://www.elsevier.com/locate/gsf)

## Research Paper

**The East Anatolia–Lesser Caucasus ophiolite: An exceptional case of large-scale obduction, synthesis of data and numerical modelling**

Y. Rolland <sup>a,b,\*</sup>, M. Hässig <sup>c</sup>, D. Bosch <sup>d</sup>, O. Bruguier <sup>d</sup>, R. Melis <sup>a</sup>, G. Galoyan <sup>e</sup>, G. Topuz <sup>f</sup>, L. Sahakyan <sup>e</sup>, A. Avagyan <sup>e</sup>, M. Sosson <sup>a</sup>

<sup>a</sup> Université de Nice Sophia Antipolis, UMR Géoazur, CNRS, IRD, Observatoire de la Côte d'Azur, 250 Rue Albert Einstein, 06560, Sophia Antipolis, France

<sup>b</sup> EDYTEM, Université de Savoie – CNRS, UMR 5204, Le Bourget du Lac, France

<sup>c</sup> Department of Earth Sciences, University of Geneva, Rue des Marâchers 13, 1205 Geneva, Switzerland

<sup>d</sup> University Montpellier, Géosciences Montpellier, UMR-CNRS-UM2 5243, Place Eugène Bataillon, 34095 Montpellier, France

<sup>e</sup> Institute of Geological Sciences, National Academy of Sciences, 24a Baghramyan Avenue, Yerevan 0019, Armenia

<sup>f</sup> İstanbul Teknik Üniversitesi, Avrasya Yer Bilimleri Enstitüsü, 34469 İstanbul, Turkey

## ARTICLE INFO

## Article history:

Received 16 April 2018

Received in revised form

9 November 2018

Accepted 19 December 2018

Available online xxx

## Keywords:

Ophiolite

Obduction

Subduction

Neotethys

## ABSTRACT

We present new, geological, metamorphic, geochemical and geochronological data on the East Anatolian–Lesser Caucasus ophiolites. These data are used in combination with a synthesis of previous data and numerical modelling to unravel the tectonic emplacement of ophiolites in this region. All these data allow the reconstruction of a large obducted ophiolite nappe, thrust for >100 km and up to 250 km on the Anatolian–Armenian block. The ophiolite petrology shows three distinct magmatic series, highlighted by new isotopic and trace element data: (1) The main Early Jurassic Tholeiites (ophiolite s.s.) bear LILE-enriched, subduction-modified, MORB chemical composition. Geology and petrology of the Tholeiite series substantiates a slow-spreading oceanic environment in a time spanning from the Late Triassic to the Middle–Late Jurassic. Serpentinites, gabbros and plagiogranites were exhumed by normal faults, and covered by radiolarites, while minor volumes of pillow-lava flows infilled the rift grabens. Tendency towards a subduction-modified geochemical signature suggests emplacement in a marginal basin above a subduction zone. (2) Late Early Cretaceous alkaline lavas conformably emplaced on top of the ophiolite. They have an OIB affinity. These lavas are featured by large pillow lavas interbedded a carbonate matrix. They show evidence for a large-scale OIB plume activity, which occurred prior to ophiolite obduction. (3) Early–Late Cretaceous calc-alkaline lavas and dykes. These magmatic rocks are found on top of the obducted nappe, above the post-obduction erosion level. This series shows similar Sr–Nd isotopic features as the Alkaline series, though having a clear supra-subduction affinity. They are thus interpreted to be the remelting product of a mantle previously contaminated by the OIB plume. Correlation of data from the Lesser Caucasus to western Anatolia shows a progression from back-arc to arc and fore-arc, which highlight a dissymmetry in the obducted oceanic lithosphere from East to West. The metamorphic *P-T-t* paths of the obduction sole lithologies define a southward propagation of the ophiolite: (1) *P-T-t* data from the northern Sevan-Akera suture zone (Armenia) highlight the presence and exhumation of eclogites ( $1.85 \pm 0.02$  GPa and  $590 \pm 5$  °C) and blueschists below the ophiolite, which are dated at ca. 94 Ma by Ar–Ar on phengite. (2) Neighbouring Amasia (Armenia) garnet amphibolites indicate metamorphic peak conditions of  $0.65 \pm 0.05$  GPa and  $600 \pm 20$  °C with a U–Pb on rutile age of  $90.2 \pm 5.2$  Ma and Ar–Ar on amphibole and phengite ages of  $90.8 \pm 3.0$  Ma and  $90.8 \pm 1.2$  Ma, respectively. These data are consistent with palaeontological dating of sediment deposits directly under (Cenomanian, i.e.  $\geq 93.9$  Ma) or sealing (Coniacian–Santonian, i.e.,  $\leq 89.8$  Ma), the obduction. (3) At Hınıs (NE Turkey) *P-T-t* conditions on amphibolites ( $0.66 \pm 0.06$  GPa and  $660 \pm 20$  °C, with a U–Pb titanite age of  $80.0 \pm 3.2$  Ma) agree with previous *P-T-t* data on granulites, and highlight a rapid exhumation below a top-to-the-North detachment sealed by the Early Maastrichtian unconformity (ca. 70.6 Ma). Amphibolites are cross-cut by monzonites dated by U–Pb on titanite at  $78.3 \pm 3.7$  Ma. We propose that the HT-MP metamorphism was

\* Corresponding author. Université de Nice Sophia Antipolis, UMR Géoazur, CNRS, IRD, Observatoire de la Côte d'Azur, 250 Rue Albert Einstein, 06560, Sophia Antipolis, France.

E-mail address: [yrolland@unice.fr](mailto:yrolland@unice.fr) (Y. Rolland).

Peer-review under responsibility of China University of Geosciences (Beijing).

coeval with the monzonites, about 10 Ma after the obduction, and was triggered by the onset of subduction South of the Anatolides and by reactivation or acceleration of the subduction below the Pontides-Eurasian margin. Numerical modelling accounts for the obduction of an "old" ~80 Myr oceanic lithosphere due to a significant heating of oceanic lithosphere through mantle upwelling, which increased the oceanic lithosphere buoyancy. The long-distance transport of a currently thin section of ophiolites (<1 km) onto the Anatolian continental margin is ascribed to a combination of northward mantle extensional thinning of the obducted oceanic lithosphere by the Hinis detachment at ca. 80 Ma, and southward gravitational propagation of the ophiolite nappe onto its foreland basin.

© 2019, China University of Geosciences (Beijing) and Peking University. Production and hosting by Elsevier B.V. This is an open access article under the CC BY-NC-ND license (<http://creativecommons.org/licenses/by-nc-nd/4.0/>).

## 1. Introduction

Ophiolites are the witness of a rare process in modern tectonics: the obduction process. Despite the paradox of being dense rock nappes transported atop lighter continental domains (e.g., Coleman, 1971, 1981; Dewey, 1976), obductions are documented in most mountain ranges around the world. Therefore, a geodynamic process has to account for this apparent paradox (Vaughan and Scarrow, 1983; Hässig et al., 2016a, b). Domains where obducted nappes are still preserved, like in Oman (Coleman, 1981; Agard et al., 2007), or in New Caledonia (Aitchison et al., 1995; Lagabrielle et al., 2013; Secchiari et al., 2017), are found in orogens which did not yet suffer a phase of intense collision. Obduction appears as a short-lived (10–20 Ma long) event, and its occurrence coincides with major plate tectonic shifts (e.g., Moores, 1982; Abbate et al., 1985; Boudier et al., 1988). However, the obduction trigger is still uncertain: may it be due to plate acceleration (Agard et al., 2007, 2014; Monié and Agard, 2009), or to other vertical forces originating from mantle upwelling (Vaughan and Scarrow, 2003; Hässig et al., 2016a, b, 2017)? Also, two contrasting models have been developed to account for obduction: (1) thrust propagation of the ophiolite on the continent via thin tectonic nappes or "flake tectonics" (Coleman, 1971; Oxburgh, 1972), or (2) continental subduction beneath an oceanic upper plate driven by slab pull (Mattauer et al., 1981; Boudier et al., 1988; Yamato et al., 2007). The contrasting views lie mostly in the fact that in the first case, the ophiolite is "actively pushed" and progresses far onto the continent without the help of slab pull in the subduction zone. The ophiolite may be further propagated by some gravitational movement above a flexural domain of the underthrusted lithosphere. In contrast, in the second case, ophiolite emplacement is a 'passive' process due to the traction of the thin passive continental margin into the subduction zone (e.g., Dewey and Bird, 1971). Many pioneering studies were led on the well-exposed Oman ophiolite, which lies on the NE edge of Arabia (e.g., Agard et al., 2007 and references therein). The Oman ophiolite is a typical example of a hot oceanic lithosphere, which formed closely before its obduction. Resulting eclogitisation of the Arabian margin suggests that continental subduction is the main process driving oceanic transport onto the continental margin (e.g., Yamato et al., 2007; Agard et al., 2014), which agrees more with the second type of obduction models. Most of the successful modelling that has been done is more in agreement with this hypothesis (Agard et al., 2014; Duretz et al., 2016). In contrast, rare models succeeded in thrusting a slice of oceanic crust onto the continent following the "active push" hypothesis (Leroy et al., 2004), and not over long distances. In this paper, we focus on the northeastern Anatolia–Lesser Caucasus (NALC) case example. This example shows that a very old obducted oceanic lithosphere at the time of its obduction (~80 Ma), could be tectonically transported over several hundreds of kilometers while presenting a resulting thickness of only several kilometers at most (Rolland et al., 2009b; Hässig et al., 2016a, b, 2017). In the following, we present new

results on the geochemistry of ophiolites from East Anatolia and Armenia and some new *P-T-t* data on the frontal part of the obducted ophiolites of the Tauride block at Hinis. In the following discussion, we reconstruct the whole obduction cycle of the Anatolian–Armenian ophiolite based on a synthesis of some selected data from Anatolia–Armenia and numerical modelling.

## 2. Geological setting

### 2.1. Geological domains

In the Lesser Caucasus and Eastern Anatolia (Figs. 1 and 2), the ophiolites were thrust towards the South by the Pontides–Transcaucasus margin of Eurasia on the Taurides-Anatolides-Platform prolonged by the South Armenian block (TAP-SAB). These two domains are briefly described below.

#### 2.1.1. The Eurasian margin (Pontides-Transcaucasus)

In the Eurasian part of the Lesser Caucasus, the basement formations are quite similar to those known all along the Eurasian margin (see reviews in Rolland et al., 2016 and Okay and Topuz, 2017). It corresponds to a Variscan basement unconformably overlain by a thick, mainly calc-alkaline, volcanogenic series of Bajocian to Santonian (170–84 Ma) age, which are the magmatic records of the north-dipping subduction of the Tethys oceanic domain below Eurasia (e.g. Adamia et al., 1977). During this period, an active continental margin domain called the Somkheto–Karabakh Island Arc occupied the northern Lesser Caucasus (Knipper, 1975; Adamia et al., 1977; Ricou et al., 1986). For details on Jurassic magmatism and geology see Galoyan et al. (2013, 2018). Onset of subduction is not well constrained. Yet, studies conducted in the Georgian (Lesser Caucasus) and the Turkish parts (Pontides) have shown simultaneous calc-alkaline magmatic activity since the Early or Middle Jurassic (e.g. Adamia et al., 1977; Hess et al., 1995; Meijers et al., 2010; Ustaömer and Robertson, 2010; Nikishin et al., 2013; Ustaömer et al., 2013; Okay et al., 2014; Rolland et al., 2016; Çimen et al., 2018). This Jurassic magmatism and coeval H-T metamorphism (Marroni et al., 2014; Okay et al., 2014) extend to the Vardar suture in the Balkans (e.g., Maffione and Hinsbergen, 2018). Early Cretaceous magmatic series are missing (e.g., Okay and Nikishin, 2015), which could result either from tectonic erosion or, rather, to a cessation of subduction during this period of time and to the onset of a new subduction set during the Cenomanian–Turonian (Okay and Şahintürk, 1997; Yılmaz et al., 1997) or Albian (Okay et al., 2006). There is a consensus concerning the end of this subduction event in the Eastern Pontides/Eastern Anatolia region and onset of continental collision of TAP-SAB with the Pontides-Transcaucasus at the transition from the end of the Late Cretaceous–Paleocene (e.g., Okay and Şahintürk, 1997; Rice et al., 2009; Meijers et al., 2017; Rolland, 2017; Sarıfakioğlu et al., 2017).

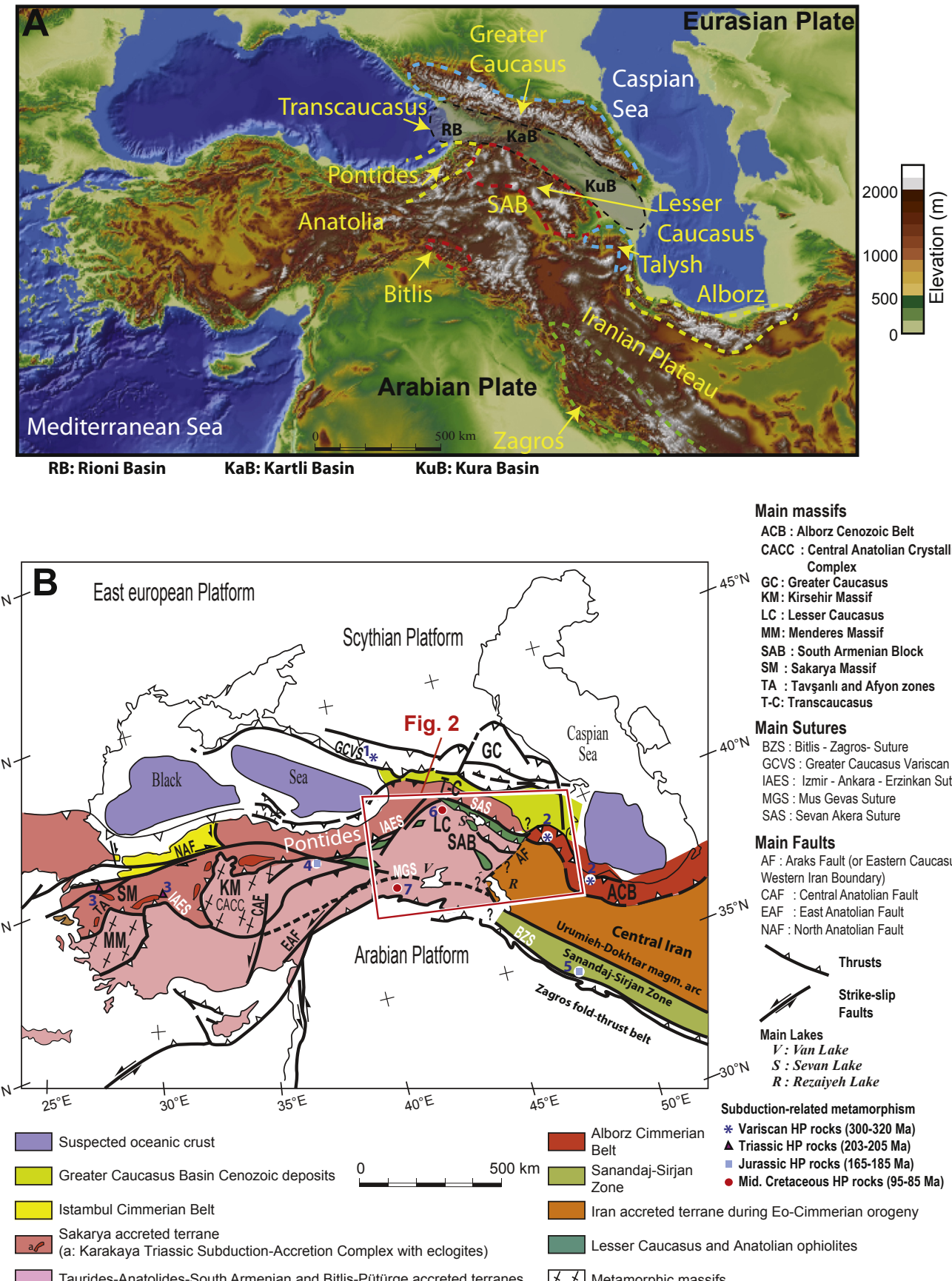


**Figure 1.** (A) Morphological map of the Middle East–Caucasus area with the main mountain belts and basins. (B) Tectonic map of the Middle East–Caucasus area, with main blocks and suture zones (modified after Rolland 2017). Location of Fig. 2 is indicated.

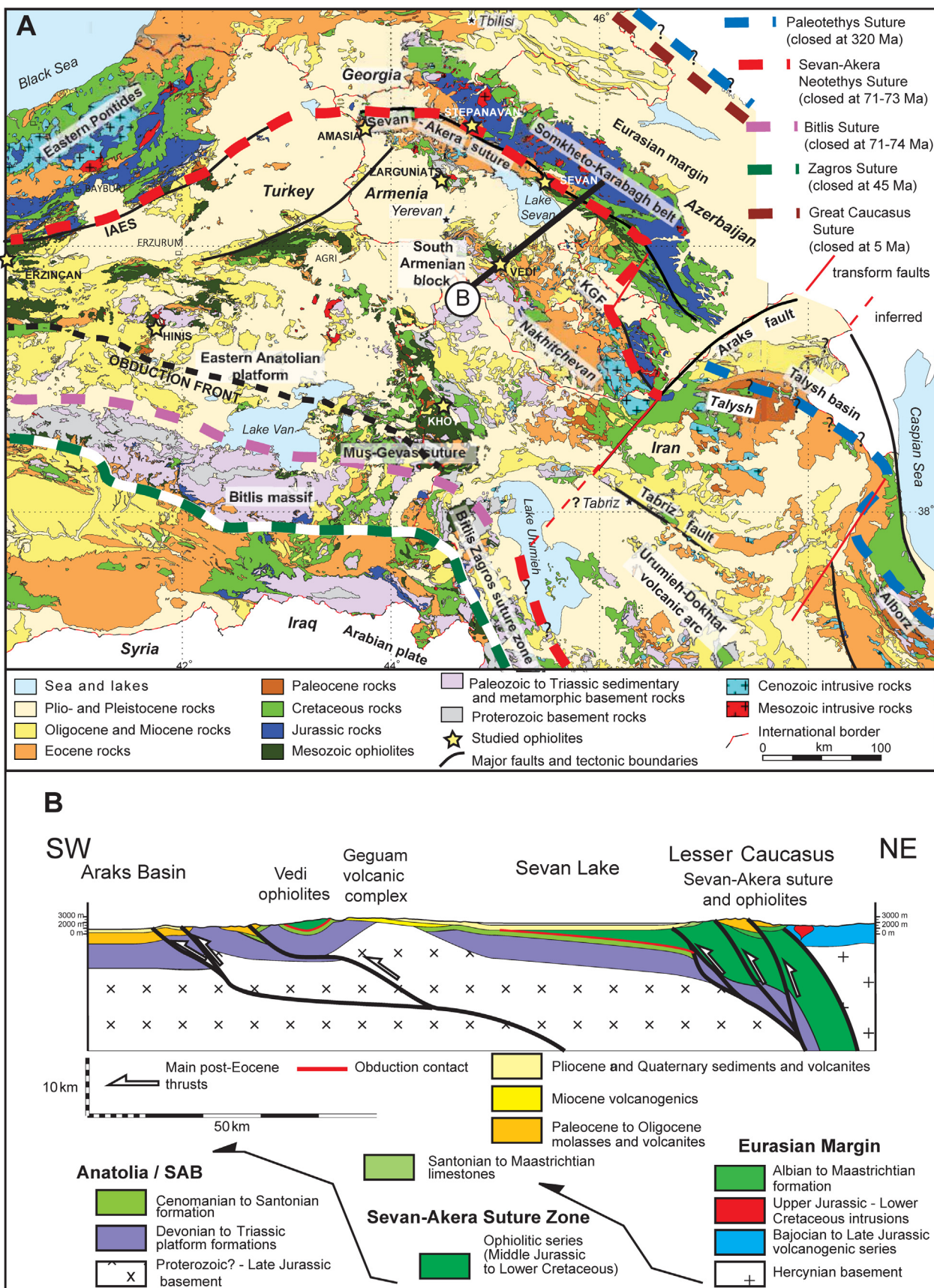


**Figure 2.** (A) Geological map of Eastern Anatolia – Armenia – Western Iran, showing the location of main units. Studied ophiolites are shown by the yellow stars. (B) Geological cross-section of the SAB-Sevan-Akera – Transcaucasus transect.

### 2.1.2. The Taurides-Anatolides-Platform and the South Armenian block (TAP-SAB)

The Tauride-Anatolide Platform (TAP) extends to the East with the South Armenian Block (SAB). This domain represents a continental platform between the northern and southern branches of Neotethys (Sengör and Yilmaz, 1981; Bozkurt and Mittwede, 2001). The TAP-SAB represents a sliver of a small continental plate detached off the northern margin of Gondwana, drifted towards the North to ultimately collide with Eurasia (Stocklin, 1974; Adamia et al., 1977; Biju-Duval et al., 1977; Dercourt et al., 1986; Şengün, 2006; Barrier and Vrielynck, 2008). Palaeomagnetic analyses indicate palaeo-latitudes for the TAP-SAB during the Early and Middle Jurassic at least 2000 km farther South than its current position (Bazhenov et al., 1996; Meijers et al., 2015). To the SE of Yerevan, the SAB series from below the obduction comprise a pile of Paleozoic to Cenomanian series, which resemble those from Gondwana (Arakelyan, 1964; Sosson et al., 2010; Danelian et al., 2014). This argues for a Gondwanian origin of the TAP-SAB, as also suggested by palaeogeographic reconstructions (Knipper and Khain, 1980; Monin and Zonenshain, 1987; Şengür et al., 1988; Robertson and Mountrakis, 2006; Barrier and Vrielynck, 2008). The rifting of the Taurides-Anatolides (including the SAB) from Gondwana is documented as initiating during Triassic times (Mart, 1987; Gealey, 1988; Kazmin, 1991).

The TAP crystalline basement crops out at Hinis, in Eastern Turkish Anatolia (Fig. 3), as a dome-shape tectonic window below the ophiolites. This basement is comprised of tourmaline-bearing leucogranites cross-cutting high-grade schists (gneisses, calc-schists and amphibolites). Topuz et al. (2017) report upper amphibolite-to granulite facies conditions for restitic migmatitic gneiss at  $\sim 0.7$  GPa and  $\sim 800$  °C at 0.7 GPa ( $2\sigma$ ), based on Ti-in-zircon temperatures of 761–831 °C, Zr-in-rutile temperatures of 775–830 °C and plagioclase-garnet-Al<sub>2</sub>SiO<sub>5</sub>-quartz geobarometry of 0.7 GPa. U-Pb dating of metamorphic zircon and rutile in the paragenesis yielded  $83 \pm 2$  Ma and  $78 \pm 3$  Ma ( $2\sigma$ ), respectively. The same authors dated the orthogenesis of the TAP basement, also by U-Pb on zircons, which yielded a Late Ordovician–early Silurian protolith age ( $444 \pm 9$  Ma,  $2\sigma$ ), whereas detrital zircons from one metaquartzite point to a Neoproterozoic–early Paleozoic provenance. These data are in good agreement with a Gondwanian origin of the Taurides (e.g., Okay et al., 2008). In addition, they mention unpublished U-Pb zircon ages of ca. 85 Ma for cross-cutting gabbros, quartz-monzonites and tonalites, which they assume to be ‘subduction-related’.

There is only one outcrop domain of the SAB crystalline basement. This basement can be seen to the North of Yerevan in Armenia (see a full description in Hässig et al., 2015, summarized below). Elsewhere, the SAB is covered by a thick Cenozoic volcanic pile (e.g., Sahakyan et al., 2017, and references therein). The basement is featured by presumed Proterozoic orthogenesis (Baghdasaryan and Ghukasyan, 1983) overlain by metapelites intruded by granodiorites. Metamorphic foliations underline a dome structure to the South of the domain. PT paths and thermobarometry on pelites from the top of the dome indicate a complex thermal history involving (1) a M1 Medium Pressure-Medium Temperature metamorphic imprint (kyanite-staurolite-garnet) culminating at 0.8–0.9 GPa and  $550 \pm 30$  °C, (2) a M2 Low Pressure-High Temperature imprint (andalusite-K-feldspar) at pressures  $<0.2$  GPa and  $600$  °C  $< T < 650$  °C, followed by (3) isobaric cooling at  $0.21 \pm 0.1$  GPa and 360–460 °C given by biotite-garnet-plagioclase thermobarometry (M3). Age for M1 is bracketed at 150–160 Ma (by Ar-Ar dating on white mica in schists and leucogranites), coinciding with granodiorite emplacement (dated by U-Pb on zircon and Ar-Ar on amphibole), and M2 is dated between 150 Ma and 130 Ma (by Ar-Ar dating on white mica). M3 is dated by

Ar-Ar on biotite at  $123.3 \pm 1.6$  Ma. The emplacement of magmatic rocks and metamorphism occurred during the top-to-N shearing, and was related to a possible South-dipping subduction.

Therefore, the metamorphic evolution of SAB is distinct from that of Hinis in the eastern Taurides-Anatolides since it does not show any evidence of the Late Cretaceous H-T metamorphism. However, similar undated extensional features as in Hinis occur in the SAB. In the SAB, extension resulted into emplacement of a thick olistolithic series along radial S-, E- and W-dipping normal faults. This extensional phase occurred closely after obduction as shown by Late Cretaceous syn-tectonic sediments in both places. In the SAB, the crystalline basement is unconformably covered by Late Cretaceous–Paleocene series dated by nanno fossils, evolving from Maastrichtian marly sandstones to Paleocene limestones (Hässig et al., 2015), as also documented in Hinis (Yilmaz et al., 2010).

During the Cenozoic, sedimentation is documented as resulting from a foreland basin context, to the North of the Arabia collision zone with TAP-SAB. Regional shortening during the Oligo–Miocene in the font of a fold-and-thrust belt lead to the formation of numerous mini-basins like the Sivas Basin (Kergaravat et al., 2016; Ribes et al., 2017). Such deformation is also recorded at Hinis, where thrusts are thought to reactivate former normal faults bounding the basement/ophiolite windows (Fig. 3). Further, three magmatic series of substantially different ages and compositions were successively emplaced in the eastern part of TAP-SAB during the Cenozoic (Rezeau et al., 2016, 2017). The protracted magmatic activity lasted 30 Myr, from Middle Eocene to Early Miocene, and is ascribed to collisional and post-collisional (extensional) magmatism, likely in response of slab melting and/or detachment (Dokuz et al., 2019), or possibly in an ongoing supra-subduction context (Sahakyan et al., 2017; Rezeau et al., 2016, 2017).

## 2.2. Nature of ophiolites

### 2.2.1. Ophiolite assemblages and oceanic environment

In Armenia and Eastern Anatolia, ophiolites are composed of, from bottom to, serpentinized peridotites intruded by gabbros, scattered cross-cutting plagiogranites in extensional shear zones, lava flows of basalt with intercalations of Middle–Late Jurassic radiolarites (ca. 180–150 Ma on gabbros and lavas, Galoyan et al., 2009; Rolland et al., 2010; Hässig et al., 2013a; Topuz et al., 2013a, b, c; 170–145 Ma on radiolarians, Danelian et al., 2007, 2008, 2010, 2012; Asatryan et al., 2010, 2012; Figs. 4 and 5). A full description of ophiolite lithologies and mineralogy can be found in Galoyan (2008), Galoyan et al. (2009), Rolland et al. (2009b, 2010); Hässig et al. (2013a, b). Structural analysis suggests that seafloor spreading was accommodated by extension along extensional faults that have exhumed deep-seated crust and mantle rocks (e.g., Mutter and Karson, 1992; Cannat, 1993). The upper mantle exhumed along normal faults consists of slightly to highly serpentinized lherzolites and harzburgites intruded by pods of cumulitic wehrlites and gabbros, which are mainly found along the extensional faults (Rolland et al., 2009b, 2010). The extensional fault surfaces were sealed by volcanic flows, in turn, covered by oceanic sediments (Fig. 6). This lithological association is typical of a slow-spreading oceanic ridge (see a review in Lagabrielle, 2009).

### 2.2.2. Age of oceanic accretion

Most ophiolites are dated to the Early to Late Jurassic, ca. 180–150 Ma, from Armenia to North-eastern Anatolia, along the Izmir-Ankara-Erzincan segment of the North Tethyan suture, and within obducted ophiolites like the Vedi klippe in Armenia (Fig. 5b). Direct dating was undertaken by Ar-Ar analyses on amphiboles from gabbros and by U-Pb analyses on zircons from plagiogranites (Zakariadze et al., 1990, 2005; Galoyan et al., 2009; Rolland et al.,

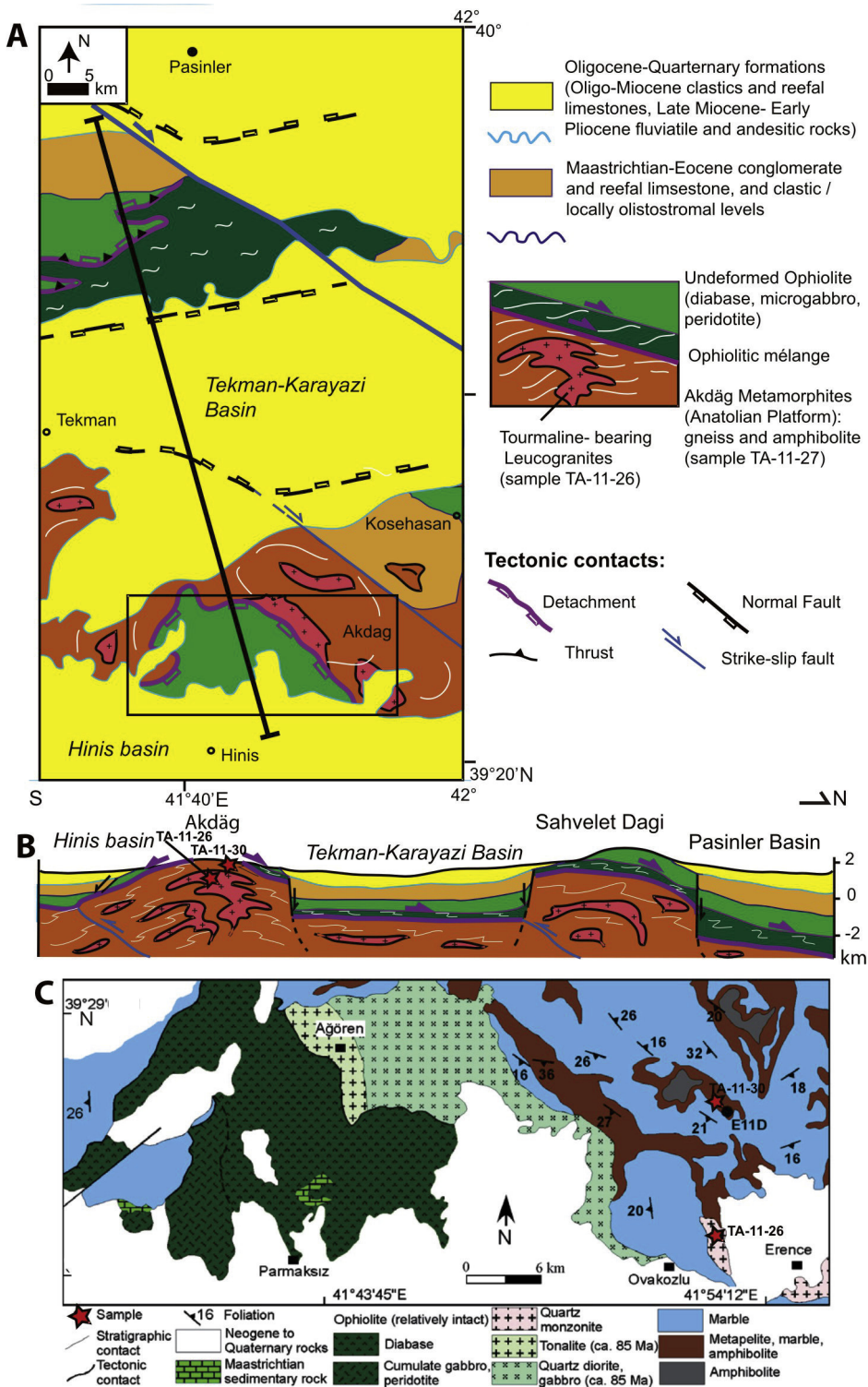


**Figure 3.** (A) Structural map of the Hinis area in Northeast Anatolia and (B) geological cross-section of the studied Akdag tectonic window (C). A, modified after Yilmaz et al. (2010) and C, modified after Topuz et al. (2017).

2010; Çelik et al., 2011; Hässig et al., 2013a; Robertson et al., 2013; Topuz et al., 2013a,b). Indirect dating on radiolarians provided similar ages (Danelian et al., 2007, 2008, 2010, 2012; Asatryan et al., 2010, 2012). For the Anatolian ophiolites, a compilation of ages can be found in Sarifakioğlu et al. (2017). Following Göncüoğlu et al. (2001), these authors highlight a more discrete group of Late Triassic–Early Jurassic ophiolitic rocks within the northern part of the

obducted nappe, along the Izmir-Ankara-Erzincan suture, with ages ranging from 208 Ma to 179 Ma, while younger ophiolitic units (Late Jurassic–Early Cretaceous) occur in the obducted series to its South. However, it is not clear if the Triassic rocks (found in a mélange unit) were generated during the continental rifting stage, or later during the drifting stage or even during the mature oceanic stage. In contrast, the Jurassic ophiolites form coherent crustal

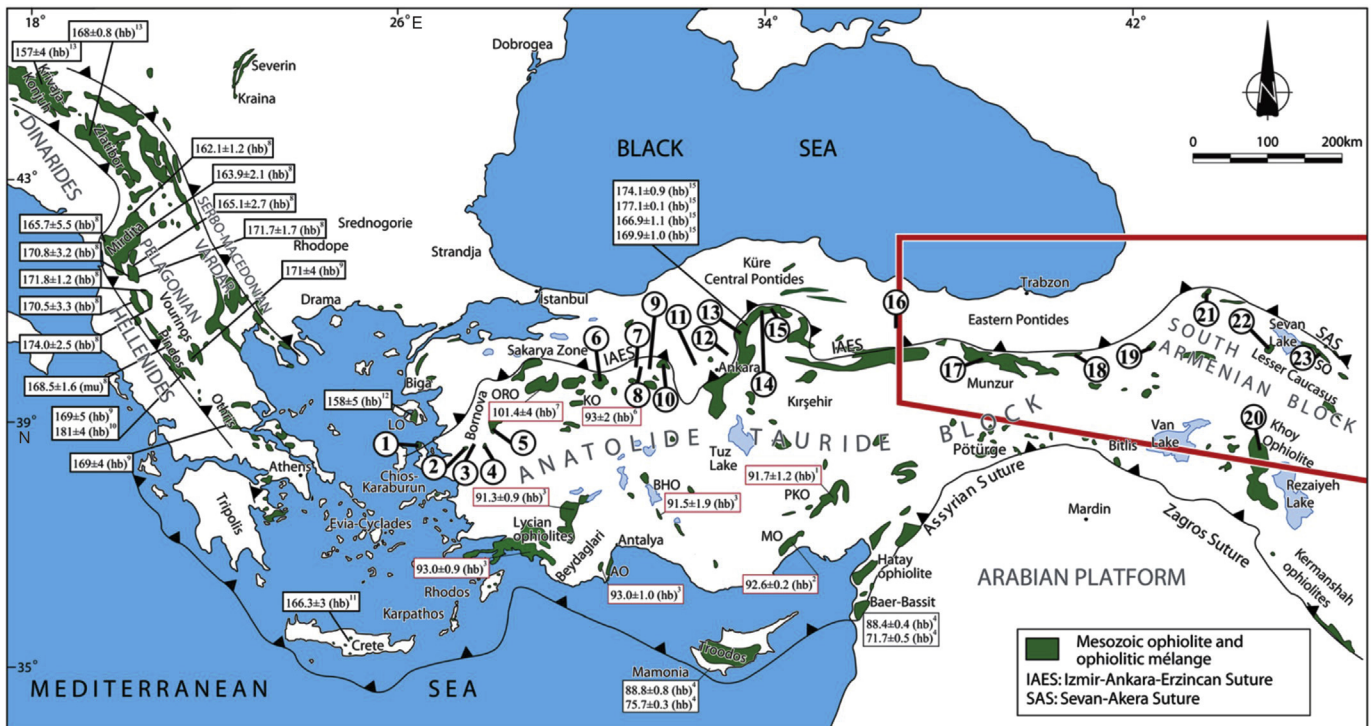


**Figure 4.** Tectonic map of Mesozoic ophiolites and ophiolitic mélanges from the Tethyan realm in Turkey and adjacent areas (modified after Stampfli et al., 2001). The bold numbers within circles indicate positioning of radiolarian biostratigraphy, radiochronology as well as magmatic rock types and metamorphic sole rock outcroppings reported in Fig. 5B. Representative geochronological data from rocks of the ophiolitic assemblages are indicated in boxes with a thin black frame, while those from metamorphic soles are indicated in boxes with a thin red frame, modified after Çelik et al. (2011). All data are from  $^{40}\text{Ar}/^{39}\text{Ar}$  analyses except where stated otherwise, numbers in exponents correspond to following references: (1) Dilek et al. (1999); (2) Parlak and Delaloye (1999); (3) Çelik et al. (2006); (4) Chan et al. (2007); (5) Galoyan et al. (2009); (6) Önen (2003); (7) Harris et al. (1994); (8) Dimo-Lahitte et al. (2001); (9) Spray et al. (1984); (10) Roddick et al. (1979); (11) Koepke et al. (2002), K-Ar age data; (12) Hatzipanagiotou and Pe-Piper (1995), K-Ar age data; (13) Lamphere et al. (1975), K-Ar age data; (15) Çelik et al. (2011). AO: Antalya Ophiolite; BHO: Beysehir-Hoyran Ophiolite; EO: Eldivan ophiolite; KO: Kinik Ophiolite; LO: Lesvos Ophiolite; MO: Mersin Ophiolite; ORO: Orhaneli Ophiolite; PKO: Pozanti-Karsanti Ophiolite; SO: Sevan Ophiolite; mu: muscovite; hb: hornblende. (\*) age data from gabbro. The thick red frame indicates the position of Fig. 5B.

units, which can be attributed to sea-floor spreading. These data support models featuring slow-spreading oceanic opening of the northern Neotethyan domain during the Lower and Middle Jurassic times, ongoing through the Cretaceous times towards the South (e.g., Robertson et al., 2013; Hässig et al., 2013b).

### 2.2.3. Formation of ophiolites in a marginal basin above a north-dipping intra-oceanic subduction zone

A Supra-Subduction Zone (SSZ) nature for the ophiolites of northeastern Anatolia and Armenia has been deduced following investigation of geochemical tendencies of magmatic rocks (e.g., Galoyan et al., 2009; Parlak et al., 2012; Hässig et al., 2013a; Topuz et al., 2013a; Fig. 7). The geochemical composition of all ophiolitic rocks from Armenia shows the presence of a subduction component in their source, but the rocks are slightly enriched with respect to Mid-Oceanic Ridge Basalts (MORBs) which has led to the interpretation of a back-arc basin environment for these rocks (Galoyan et al., 2007, 2009; Rolland et al., 2009b, 2010; Hässig et al., 2013a, 2017). A relatively similar trend is observed in Anatolia all along the Izmir-Ankara suture and in the obducted ophiolites, although a fore-arc environment is defined in the southern younger part of the ophiolite nappe, inferred from the boninitic chemical signatures of basalts and gabbros (Parlak et al., 2012; Sarifakioğlu et al. (2017)). Both scenarios, fore- or back-arc origin, can be reconciled by reconstructing a North-dipping intra-oceanic subduction, with younging ages, and fore-arc rocks to the South of the Neotethyan domain (e.g., Göncüoğlu, 2010; Sarifakioğlu et al., 2017). This, in turn, suggests a southward retreating slab by roll-back

process (Galoyan et al., 2009; Rolland et al., 2010, 2011). These data also suggest the existence of an intra-oceanic arc. There is still no clear evidence for any intra-oceanic arc preserved in the ophiolite sequence. However, the metamorphic series found directly North of Erzincan, below the ophiolite, are thought to represent a deformed arc series (Güçer et al., 2007; Aslan et al., 2011; Güçer and Aslan, 2014). Geochemical analyses show that these Erzincan metamorphic rocks consist of meta-basalts and meta sediments with tholeiitic to calc-alkaline affinities (Güçer et al., 2007; Güçer and Aslan, 2014). These geochemical tendencies argue for the occurrence of a volcanic arc between the passive continental margin of the TAP-SAB to the South and the oceanic domain to be obducted over it, from the North.

The presence of an intra-oceanic subduction in the Neotethys domain to the South of the Eurasian margin implies that two subduction zones were active at the same time as an active margin existed along the Pontides and transcaucasus regions (the so-called Somkheto–Karabakh Island Arc, see section 2.1.1.) during the Early–Middle Jurassic (e.g., Yalıniz et al., 2000; Göncüoğlu, 2010). Most authors propose that the two subductions were both North-dipping, although South-dipping intra-oceanic subduction might be possible as well (Galoyan et al., 2018).

### 2.2.4. The alkaline volcanic series

Pillow-basalts with an Ocean Island Basalt (OIB) alkaline composition lie on top of the ophiolite series in Armenia (Galoyan et al., 2007, 2009; Rolland et al., 2009b, 2010; Hässig et al., 2013a), and in NE Turkey as well (e.g., Parlak et al., 2012 and Sarifakioğlu

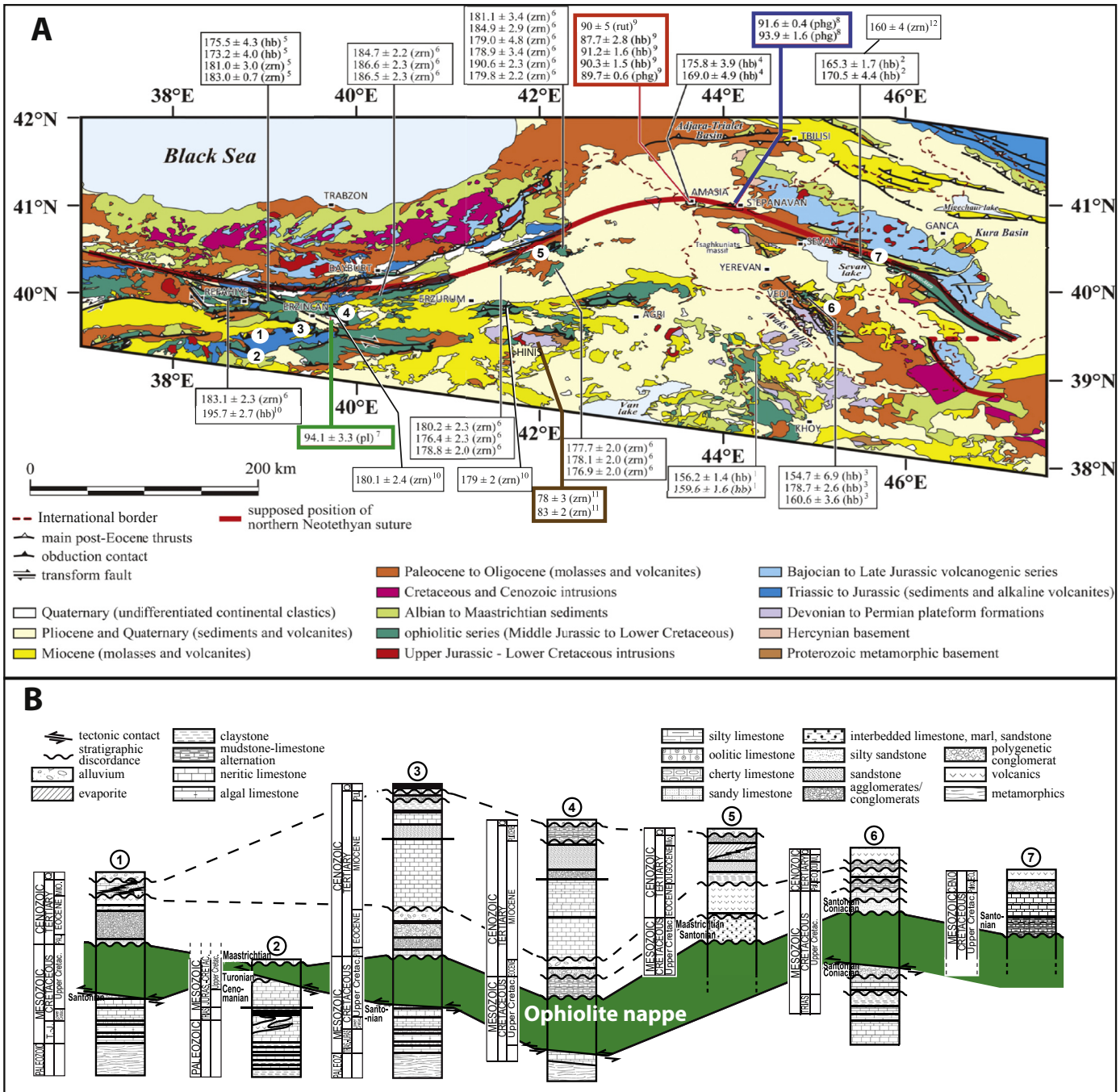


**Figure 5.** (A) Structural map of the Lesser Caucasus-Eastern Pontides-Northeast Anatolides regions, modified after Hässig et al. (2017). The ages indicated are from ophiolites (thin black frame), metamorphic soles (bold red frame), Greenschist facies (bold green frame), HP units (bold blue frame), and HT domain (bold brown frame). References to ages are: (1) Pessagno et al. (2005), (2) Galoyan et al. (2009), (3) Rolland et al. (2010), (4) Hässig et al. (2013a), (5) Topuz et al. (2013a), (6) Robertson et al. (2013), (7) Aslan et al. (2011); Gücer and Aslan (2014), (8) Rolland et al. (2009a) and (9) Hässig et al. (2019), (10) Sarıfakıoğlu et al. (2017), (11) Topuz et al. (2017), (12) Zakariadze et al. (1990). (B) Compilation of chronological data including extension of the radiolarian fauna, magmatic series of the ophiolite bodies outcropping emplaced prior to the obduction event and metamorphic lithologies marking the limit between the ophiolites and the Eurasian margin as well as between the ophiolites and the underthrusted TAP-SAB margin from the Izmir-Ankara-Erzincan and Sevan-Akera sutures including the Bornova Zone and the Karaburun Peninsula, modified after Hässig et al. (2013b). Locations of numbers 1–7 are shown in Fig. 4A: (1), (3) and (4) modified after Gedik (2008); (2) modified after Moix et al. (2008); (5) modified after Bozkuş (1998); (6) and (7) modified after Sokolov (1977).

et al., 2017; Hässig et al., 2013b for reviews; Fig. 7). Such occurrences of volcanism are widespread, though of variable thickness, in the various ophiolite locations, throughout the Ankara-Erzincan suture (e.g., Sarıfakıoğlu et al., 2017). The age and relationships of alkaline lavas with respect to the ophiolites is not always clear in the western part of the IAESZ, but can be bracketed from the late Bathonian to the early Aptian (165–125 Ma;

Göncüoğlu et al., 2006). These alkaline rocks are found directly above an unconformity on top of the ophiolite body in Armenia, outcropping as fresh and large (meter-scale) pillow lavas interbedded in pelagic limestones and sometimes in radiolarites (Fig. 6), dated at 117 Ma (mid-Early Cretaceous) by Ar-Ar on amphibole by Rolland et al. (2009b). This age was later confirmed by radiolarian biostratigraphy (Danelian et al., 2012, 2014). Along

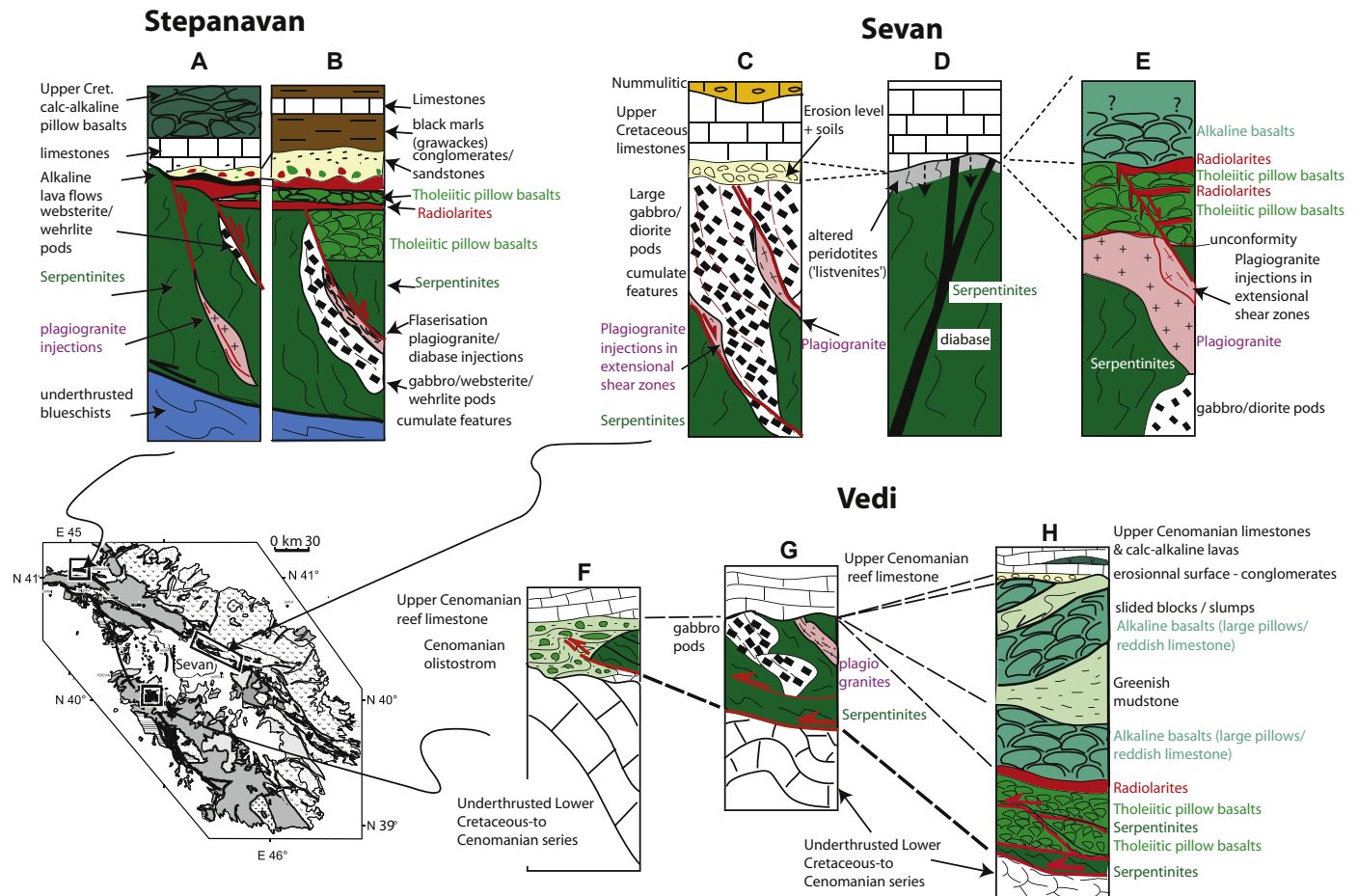


**Figure 6.** Synthetic logs of ophiolite sections from Armenian ophiolites, modified after Rolland et al. (2009b).

the Sevan-Akera suture zone, radiolarians intercalated with mafic volcanic rocks exhibit latest Tithonian to late Valanginian ages (135–123 Ma) (Asatryan et al., 2012). In the Karabagh and Amasia areas OIB lavas are bracketed by late Barremian to early Aptian (~113 Ma; Asatryan et al., 2011) and Cenomanian (96–92 Ma; Danielian et al., 2014) radiolarians. These ages substantiate long lasting volcanic activity throughout the Early Cretaceous (123–92 Ma), after a >30 Myr period of magmatic inactivity on the ocean floor. The geochemical signature of these lavas seems unrelated to subduction (Galoyan et al., 2007, 2009; Rolland et al., 2009b, 2010; Hässig et al., 2013a,b). However, the widespread occurrence of this magmatism at regional scale throughout the Early Cretaceous is likely to have significantly re-heated the Northern Neotethys oceanic lithosphere, which changed its buoyancy and may be an explanation for obduction (Rolland et al., 2009b; Hässig et al., 2015, 2016a, b), as it will be discussed in section 4.4 on the basis of numerical modelling.

#### 2.2.5. The calc-alkaline series

In Stepanavan, in the northwestern part of the Armenian obducted nappe, a series of pillow lavas with compositions ranging from calc-alkaline basalts to andesites, originates from a subduction-related mantle source (Galoyan et al., 2007; Rolland et al., 2009a,b; Fig. 7). There, the volcanic series is very thick ( $\geq 800$ –1000 m). It was emplaced in submarine conditions above an unconformity on top of the ophiolite, marked by an erosional level and Coniacian–Santonian conglomerates overlain by reef limestones (Fig. 6). In Amasia, Late Cretaceous series with

limestones and intercalated volcanic tuffs also occur, overlain by Late Maastrichtian–Paleocene unconformity (Hässig et al., 2013a), which shows a probable lateral extension of these series. Thus, the stratigraphic relationships in Amasia and Stepanavan indicate a maximum age of these series in the Coniacian–Santonian, and a minimum age before the Late Maastrichtian–Paleocene. This series is thus bracketed between 89 Ma and 66 Ma and is interpreted as featuring a volcanic arc resulting from a subduction stage, which would have started in this time range.

#### 2.2.6. The 'mélange' unit(s)

The mélanges found under the un-metamorphosed ophiolitic units are represented either by (1) a sedimentary mélange (Huene et al., 2004; Vannucchi et al., 2008; Festa et al., 2010), or (2) tectonic mélanges (Cloos and Shreve, 1988; Dilek and Whitney, 1997; Elitok and Drüppel, 2008).

- (1) The presence of a sedimentary mélange, is well exemplified in the Vedi area in the frontal part of the obducted nappe, where rounded blocks of ophiolite are found interbedded in a fine-grained chlorite-rich matrix (Sosson et al., 2010). This is taken as an evidence for a sedimentological environment for the mélange.
- (2) In most places, the mélanges found below the ophiolite are mostly tectonic in character, as described in Hässig et al. (2013a). Direction of tectonic transport during obduction is in agreement with a NNE–SSW stretching direction and a general top-to-the-South sense of shear. The metamorphic grade of the

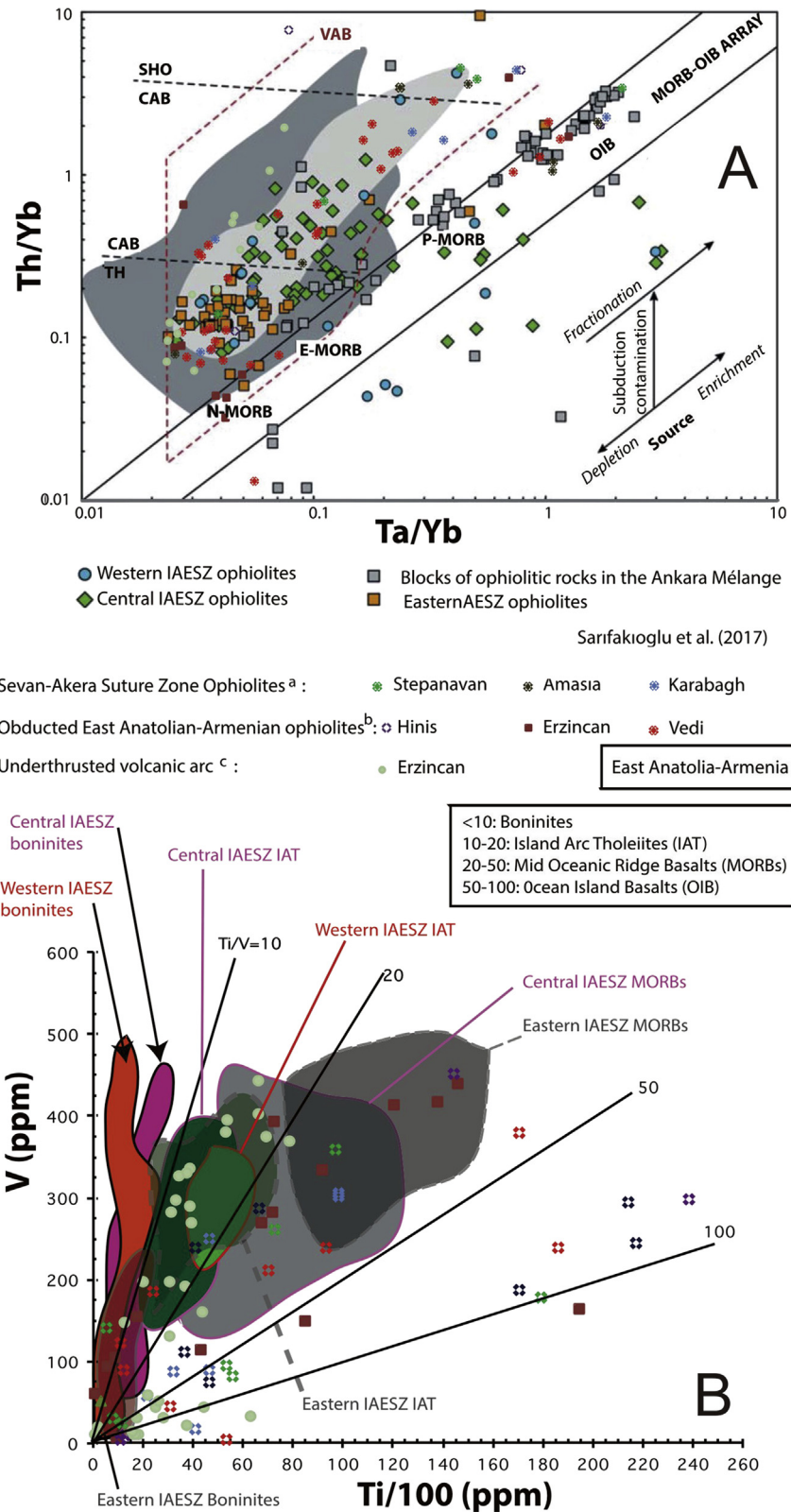


**Figure 7.** (A) Th/Yb versus Ta/Yb diagram (Pearce et al., 1984) for comparison of ophiolite rocks from Anatolia-Armenia regions. Data from Anatolia are compiled from Sarifakioğlu et al. (2017). Light-grayfield represents basaltic rocks from the Amasia, Stepanavan, and Sevan ophiolites (Galoyan et al., 2007, 2009; Rolland et al., 2009a, b, 2010; Hässig et al., 2013a, b). Dark-gray field marks basaltic rocks from the Vardar suture zone (Koglin, 2008). Data from Eastern Anatolia-Armenia are from (reference numbers in exponents): a, Galoyan et al. (2007, 2009); Hässig et al. (2013a); b, Rolland et al. (2009b, 2010); Hässig et al. (2013b); c, Gücer et al. (2007). Note that similar rock types including OIB-type rocks occur from West and Central IAESZ (İzmir Ankara Erzincan Suture Zone) to Eastern Anatolia and Lesser Caucasus CAB: calc-alkaline basalts; E-MORB: enriched mid-ocean-ridge basalt; N-MORB: normal-mid-ocean-ridge basalt; OIB: oceanic-island basalt; P-MORB: plume mid-ocean-ridge basalt; SHO: shoshonitic basalts; TH: tholeiitic basalts; VAB: volcanic-arc basalt. (B) Ti/100 vs. V diagram (Shervais, 1982). Fields for IAESZ ophiolites are from Sarifakioğlu et al. (2017) and references therein and data from Eastern Anatolia-Armenia as for above. Note the presence of boninites clearly evidenced only in West and Central IAESZ, while the Eastern Anatolian IAT and MORB-type ophiolites overlap with the West and Central IAESZ. OIB-type rocks from West and Central IAESZ are not shown for clarity.

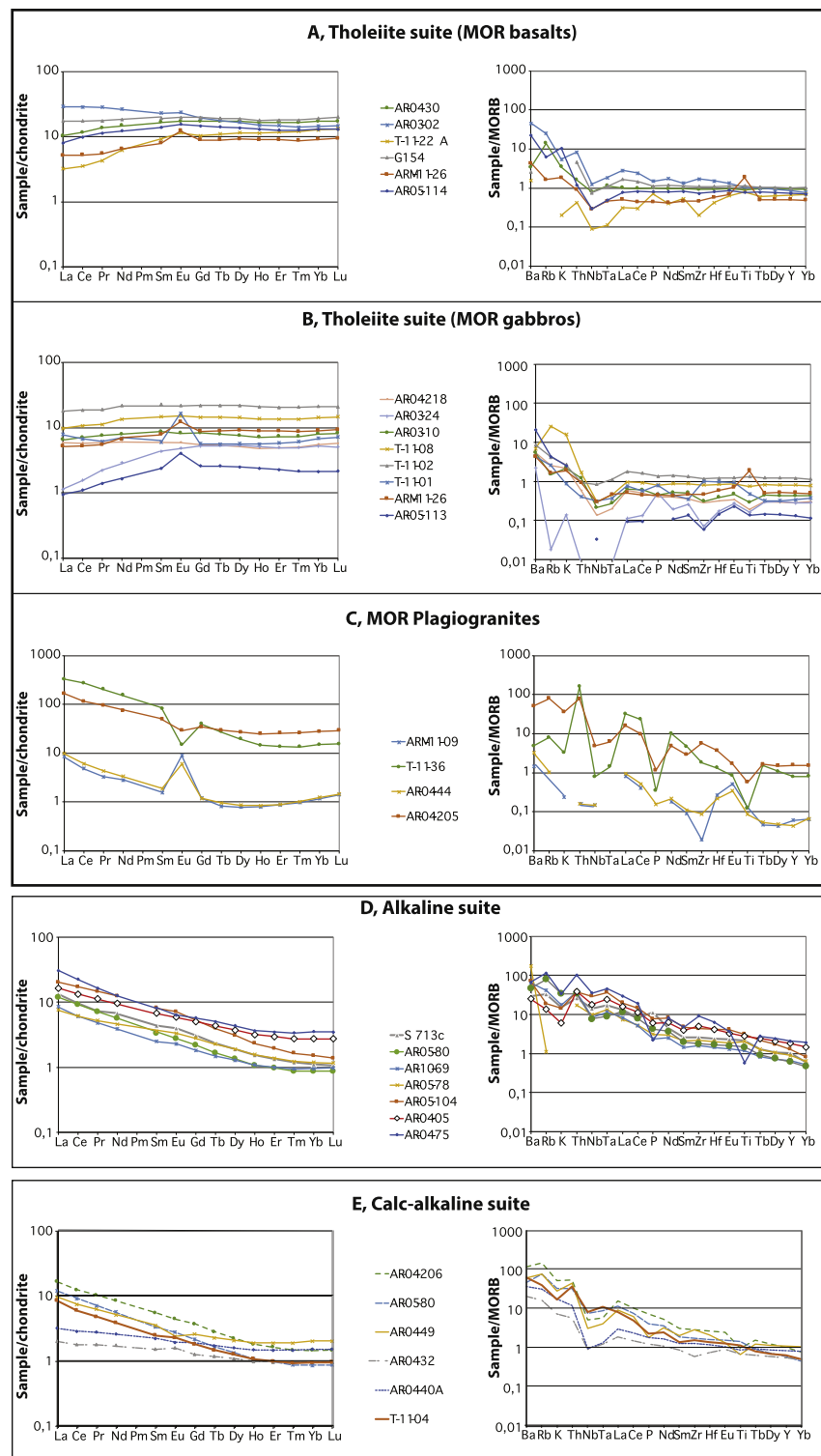
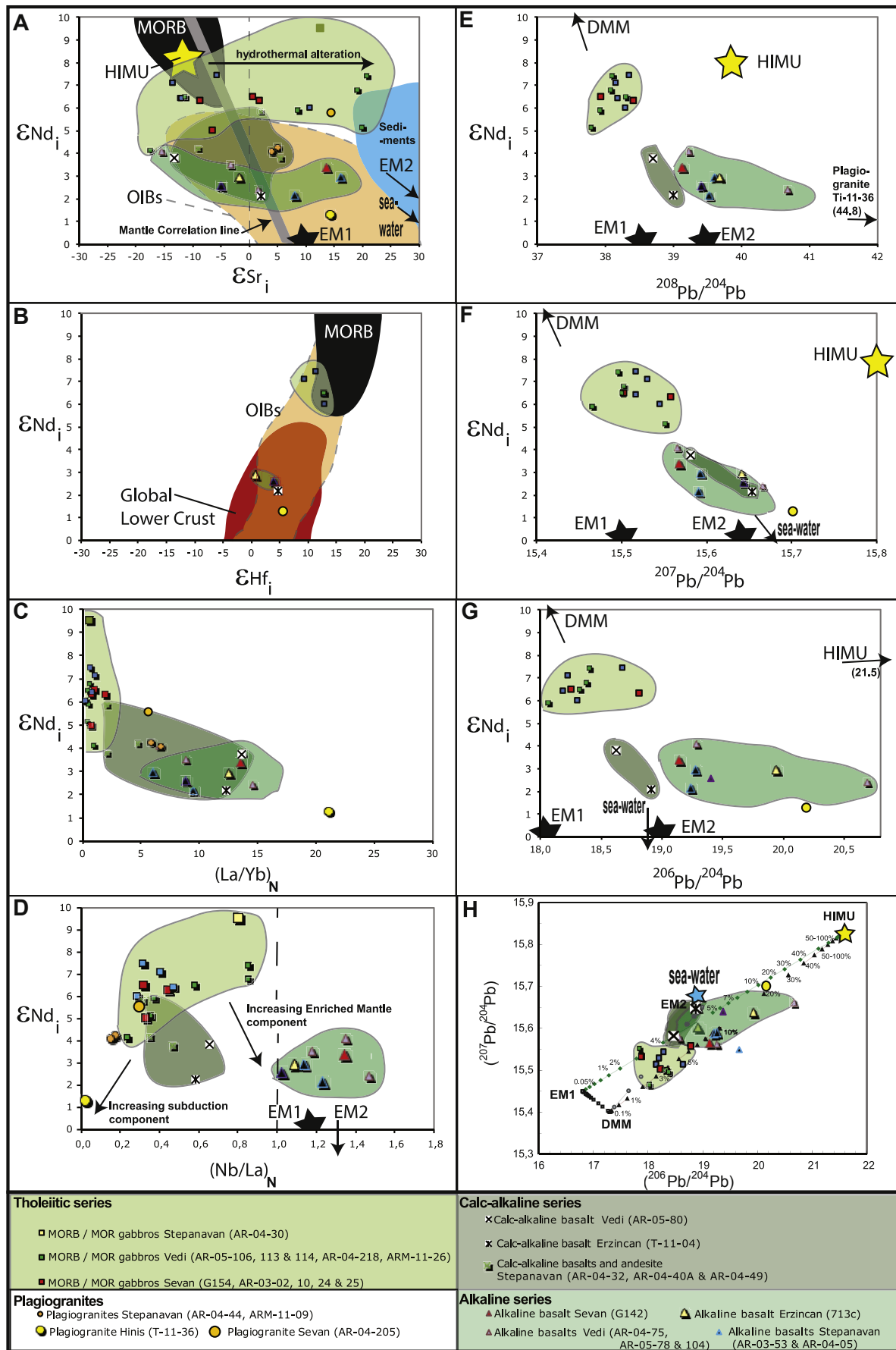


**Figure 8.** Representative rare earth and trace element patterns of each magmatic suite from the East Anatolian – Armenian ophiolites (see data in [Supplementary Table 1](#)). Left, rare earth element (chondrite-normalized) diagrams and right, extended trace element (MORB-normalized) spidergram patterns. Normalization values are after [Evensen et al. \(1978\)](#) and [Sun and McDonough \(1989\)](#).

mélange is mostly in the greenschist facies, while it locally includes km-sized lenses of garnet-amphibolites. The geochemical composition of part of the metamorphic units beneath the Stepanavan, Amasia and Hinis ophiolites shows several geochemistries as for the non-metamorphic ophiolite

alkaline affinity similar to the alkaline oceanic island basalts (OIB) suite emplaced on top of the ophiolite, a slightly subduction-modified tholeiitic affinity similar to the ophiolite gabbros and basalts, and pure N-MORB ([Hässig et al., 2019](#); Galoyan, pres. comm.).



### 2.2.7. Degree and age of metamorphism of underthrusted metamorphic units

A compilation of ages of underthrusted metamorphic units, from below the ophiolite is presented on Fig. 5.  $^{40}\text{Ar}/^{39}\text{Ar}$  ages for the metamorphism of the greenschist facies volcanic sequence underthrusted below the Refahiye ophiolite North of Erzincan have been obtained by Gücer and Aslan (2014) for (albitic) plagioclase populations, which yield ages of  $100.8 \pm 3.4$  Ma (Albian) and  $94.1 \pm 3.3$  Ma (Cenomanian). These ages are tentatively interpreted as those of the greenschist-facies metamorphic recrystallization of the rocks (at  $\sim 320\text{--}350^\circ\text{C}$  and 0.4 GPa according to preliminary estimates; Gücer and Aslan, 2014), which are globally similar to those along the Sevan-Akera suture zone.

In the Stepanavan metamorphic unit (NW Armenia), a HP metamorphic unit is found below the non-metamorphic obducted ophiolite nappe. This unit exhibits metabasites and schists representing a deep accretionary prism including eclogites ( $1.85 \pm 0.02$  GPa and  $590 \pm 20^\circ\text{C}$ , Hässig et al., 2019) and blueschists ( $1.2 \pm 0.1$  GPa,  $550 \pm 20^\circ\text{C}$ ; Rolland et al., 2009a) dated by Ar-Ar on phengite at 95–91 and partially reset in greenschist facies at 71 Ma (Rolland et al., 2009a). These conditions feature the onset of an intra-oceanic subduction zone in the Cenomanian times, and a second phase of deformation during exhumation in the Maastrichtian times. In the Amasia (NW Armenia) the garnet amphibolites embedded in the tectonic mélange of the obduction sole, exhibit MP-HT conditions of  $0.65 \pm 0.05$  GPa and  $600 \pm 20^\circ\text{C}$ . datings on this unit are featured by similar within error Ar-Ar ages on phengite and amphibole and U-Pb on rutile bracketed within 91–88 Ma (Hässig et al., 2019).

## 3. Results

### 3.1. Geochemistry of the obducted nappe magmatic series

In this paper, we report new major, trace and isotope element data. The analytical procedures are displayed in Suppl. Material 1 and the data is displayed on Supplementary Tables 1 and 2 and Figs. 8 and 9. We selected representative samples of each of the magmatic suites (described in section 2.2).

#### 3.1.1. Major-trace-REE geochemistry

In agreement with previous works of Galoyan (2008), Galoyan et al. (2009), Rolland et al. (2009b) and Hässig et al. (2013a, b, 2017), the following main geochemical tendencies are observed in analysed samples.

**3.1.1.1. Major element data.** The geochemical analyses of the ophiolitic rocks from the East Anatolian-Armenian area are of relatively alkaline composition in comparison to MORB. Major element data of pillow- lavas and gabbros show that they have predominantly basalt to trachybasalt compositions. Major element analyses of plutonic rocks ranges from gabbros to granites (*plagiogranites*) with intermediate dioritic compositions (Supplementary Table 1). These magmatic rocks appear to plot in a large domain comprised between alkaline and tholeiitic tendencies of the TAS diagram while in the AFM diagram most rocks lie close to the limit between the tholeiitic and calc-alkaline fields. Main features are pointed below: This large compositional range is ascribed to the presence of three distinct series, referred below as

(1) the ophiolitic suite; (2) the alkaline suite and (3) the calc-alkaline suite.

- (1) Overall, the rocks of the ophiolitic tholeiite suite are enriched in MgO and more depleted in TiO<sub>2</sub>, K<sub>2</sub>O and P<sub>2</sub>O<sub>5</sub> relative to the alkaline and calc-alkaline suite (Supplementary Table 1). The volcanic rocks from the different studied areas plot in the same compositional range (from basalts to andesites and trachyan-desites), and are relatively richer in Na<sub>2</sub>O than the plutonic rocks of the same series.
- (2) The studied alkaline lavas from different zones plot in the same range, varying compositionally from basanite-trachybasalt to basaltic trachyandesite and trachyandesite, and are clearly calc-alkaline/alkaline in composition. One of the most significant features of the alkaline lavas is their higher TiO<sub>2</sub>, K<sub>2</sub>O and P<sub>2</sub>O<sub>5</sub> contents.
- (3) The arc-type calc-alkaline lavas, having trachybasalt and basaltic trachyandesite compositions in TAS diagram, plot essentially in a transitional position between ophiolitic and alkaline domains, except for lower TiO<sub>2</sub> and higher Al<sub>2</sub>O<sub>3</sub> contents, which depend on the abundance of plagioclase in such rocks.

Thin section observations and previous studies of the Armenian ophiolites (e.g., Palandjyan, 1971; Abovyan, 1981; Ghazaryan, 1994; Galoyan et al., 2007, 2009; Rolland et al., 2009b, 2010) have shown that the whole magmatic sequence has been affected by oceanic low-temperature hydrothermal alteration events. These processes induced modification of the whole-rock chemistry, as revealed by high LOI values (Supplementary Table 1).

**3.1.1.2. Trace elements.** Trace element contents (Fig. 8) confirm the presence of three clearly distinct magmatic suites, as defined in the previous section.

- (1) Basalts and gabbros of the ophiolite tholeiite suite (Fig. 8A,B) show strong enrichments in LILE (Large Ion Lithophile Elements: Ba, Rb, K, Th), close and up to ten times MORB values. Plagiogranites have a larger compositional field, with LILE up to hundred times N-MORB values (Fig. 8C). Though, they share similar geochemical tendency with gabbros and basalts, and are therefore thought to derive from gabbros through fractional crystallisation processes. Basalts, gabbros and plagiogranites bear negative anomalies in Nb-Ta and Ti, which is generally indicative of volcanic island arc environments (e.g., Taylor and McLennan, 1985; Plank and Langmuir, 1998).
- (2) Overall, the concentrations of each element in the alkaline basalts exceed the concentrations in the basalts from ophiolitic tholeiite series (Fig. 8D). Moreover, alkaline series basalts are characterized by high abundances of LILE (10–100 times those of N-MORB), high field strength elements (Nb, Ta, Zr and Ti), and light rare-earth elements (LREE).
- (3) The calc-alkaline suite rocks show strong depletions in Nb and Ta, relative to Th and La, and slight Ti negative anomalies (Fig. 8E). They globally show stronger enrichments in LREE and LILE than the ophiolite suite rocks (10 to 100 times those of N-MORB).

These differences in normalized element patterns may reflect either (i) some local-scale mantle heterogeneities, which may

**Figure 9.** Isotopic data obtained on the East Anatolian – Armenian ophiolite magmatic suite (see data in Supplementary Table 2). Compositions of The MORB and OIB fields, and the trend towards crustal values are from the GEOROC database [<http://georoc.mpcn-mainz.gwdg.de/georoc/>]. Mantle end-members are after Hart (1984); Zindler and Hart (1986) and Sun and McDonough (1989). Compositions of modern marine sediments after Othman et al. (1989). Sr, Nd and Pb seawater isotopic composition is after Piepras and Wasserburg (1987), Palmer and Edmond (1989), Tachikawa et al. (1999) and Abouachami and Goldstein (1995).

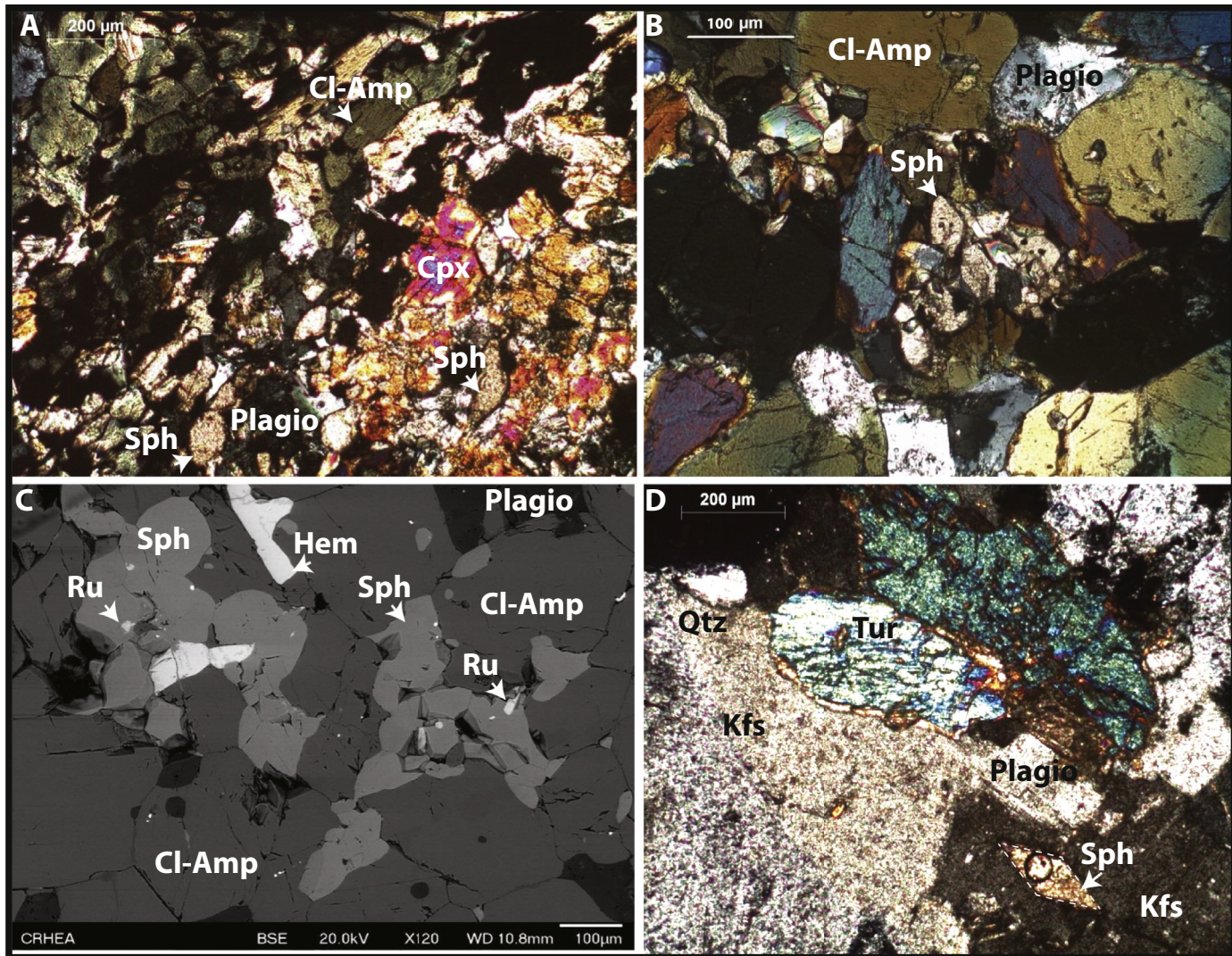


**Figure 10.** Photomicrographs of Hinis Akdag metamorphics: amphibolite (T-11-30) (A-C), and leucogranite/quartz-monzonite (T-11-26) (D). (A) photo in crossed polars showing the resorption of clinopyroxene (Cpx), which recrystallized into the main Hornblende amphibole (Cl-Amp) + plagioclase (Plagio) assemblage. (B) Titanite (or Sphene, Sph) occurs as sub-hedral or anhedral patches, with clear-cut rectilinear mineral boundaries to amphiboles (photo in crossed polars). (C) back-scatter SEM image of a titanite + hematite (Hem) aggregate showing inclusions of rutile (Ru). Note the unzoned nature of titanite. (D) photo of sample T-11-26 tourmaline (Tur) bearing leucogranite in crossed polars. Titanite has a perfect euhedral shape, and occurs as inclusions within large K-feldspar (Kfs) grains, and is thus part of the magmatic crystallization sequence which ends with tourmaline and quartz (Qtz).

control the composition of magmas (e.g., Saccani et al., 2015; Bortolotti et al., 2018) or (ii) some distinct tectonic environments. As suggested by Warren (2016) and references therein, there is increasing evidence that chemical heterogeneities affect very large portions of the mantle (>150 km). (ii) However, as suggested by evolving geochemical composition through time these trends rather support that these rocks of the three series are not petrogenetically related and most likely derived from melts formed in different tectonic settings: (1) N-type MORB (and/or BABB) for the tholeiitic series, (2) Ocean-island and/or within-plate alkali basalts for the alkaline series and (3) volcanic island arc for the calc-alkaline series.

### 3.1.1.3. REE geochemistry

(1) In the chondrite-normalized rare earth element (REE) diagrams, analysed ophiolite tholeiitic basalts and gabbros have flat and parallel REE patterns in chondrite-normalized plots ( $[\text{La/Yb}]_{\text{N}} = 0.6\text{--}0.9$ ), showing some slight depletions in LREE

and a slight enrichment in MREE (Fig. 8A,B). No extensive Eu anomalies were observed ( $\text{Eu/Eu}^* = 0.95\text{--}1.15$ ), which shows that plagioclase has not been fractionated, and is enriched in the final liquid. The concentration of REE for volcanic rocks ranges from 8 to 30 times chondrite and for gabbros from 1 to 15 times chondrite, except for a flaser gabbro—60 times (sample AR-03-25). These features are interpreted as a result of extreme crystal fractionation involving plagioclase, clinopyroxene, orthopyroxene and, to a lesser extent, olivine accumulation (Pallister and Knight, 1981), with some possible enrichment from shear zone fluids for sample AR-03-25. The REE patterns of plagiogranites (Fig. 8C) show significant enrichments in LREE as compared to gabbros. They show two distinct cases: (i) a very significant LREE-MREE enrichment, up to 300 times chondrite values for the lightest REEs, and negative Eu anomalies, or (ii) a very slight LREE enrichment (up to 10 times chondrite values) for the two plagiogranites from Stepanavan (sample AR-04-44, ARM-11-09). These latter samples are characterized by a greater depletion in the middle to heavy REE

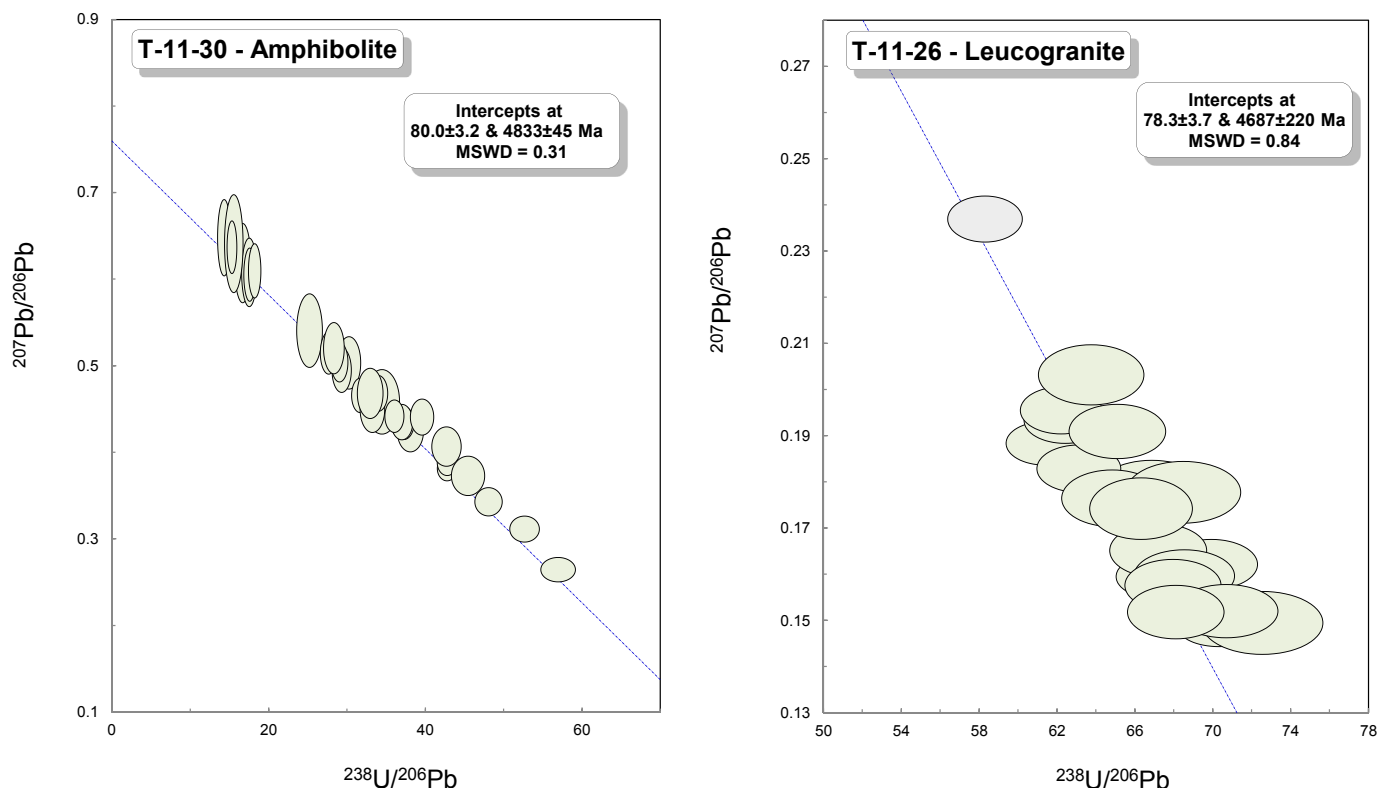


**Figure 11.** U-Pb titanite geochronological data of Hinis amphibolite (T-11-30) and leucogranite/quartz-monzonite (T-11-26). Ages are given at  $2\sigma$ ; data-point error ellipses are at 68.3% conf. ( $1\sigma$ ).

compared to other plagiogranites, and strongly positive Eu anomalies ( $\text{Eu/Eu}^* = 4.05$ ) that is ascribed to high plagioclase contents due to their cumulative nature.

- (2) In contrast, chondrite-normalized REE patterns of alkaline lavas (Fig. 8D) show huge LREE enrichments versus HREE ( $(\text{La/Yb})_N = 6\text{--}14$ ), being characteristic of intraplate continental basalts, as compared to ophiolite lavas. Meanwhile, no extensive Eu anomalies were observed ( $\text{Eu/Eu}^* = 0.95\text{--}1.15$ ). The pattern of a trachydacite sample (AR-04-75) is parallel to those of the basanite-trachyandesite series having the highest overall REE concentration.
- (3) Chondrite-normalized REE patterns of calc-alkaline lavas are strongly parallel and form a narrow domain (Fig. 8E). They have similar HREE contents similar to volcanics of previous series and display significantly more depleted to similar LREE contents as compared to alkaline series rocks ( $(\text{La/Yb})_N = 2.1\text{--}10$ ).

These differences of trace element behaviours between the three studied series further support that these rocks are petrogenetically unrelated and, most likely derived from melts formed in different tectonic settings.

### 3.1.2. Nd, Sr, Hf, Pb isotope geochemistry

**3.1.2.1. Tholeiite ophiolite series.** Initial  $\varepsilon_{\text{Nd}_{\text{I}}}$  values of the ophiolitic tholeiites lavas from the different studied zones range from +5.9 to +9.5 (Supplementary Table 2). They are intermediate between typical values of MORBs and OIBs (Fig. 9A,B). The gabbros have  $\varepsilon_{\text{Nd}_{\text{I}}}$  (+4.3 to +6.5) and Sr isotopic values (0.70386–0.70557) in the same range as volcanic rocks. The Pb isotopic ratios in ophiolitic

tholeiites (gabbros and basalts) range from 37.8 to 38.5 for  $^{208}\text{Pb}/^{204}\text{Pb}$ , from 15.46 to 15.57 for  $^{207}\text{Pb}/^{204}\text{Pb}$  and from 18.0 to 18.7 for  $^{206}\text{Pb}/^{204}\text{Pb}$  (Fig. 9E–H). In all the isotope diagrams both volcanic and plutonic rocks overlap, or plot close to the N-MORB domain. Both gabbros and basalts indicate a source region that experienced long-term depletion in LREE (Fig. 9C). A trend towards lower ( $\text{Nb/La}$ ) ratios with increasing degrees of fractional crystallization (from basalts to plagiogranites), suggests an increased contamination by subduction fluids for more differentiated terms in the series. The  $(^{87}\text{Sr}/^{86}\text{Sr})_{\text{i}}$  ratios range from 0.7037 to 0.7057 for these rocks, which is significantly too high for typical tholeiitic MORB lavas. These values are thus not considered as their primary mantle-derived magmatic Sr isotope signature (Fig. 9A). This shift towards high  $^{87}\text{Sr}/^{86}\text{Sr}$  radiogenic ratios is commonly attributed to exchange between rocks and seawater during oceanic crust hydrothermal alteration (e.g., McCulloch et al., 1981; Kawahata et al., 2001; Bosch et al., 2004). Moreover, this increase of  $(^{87}\text{Sr}/^{86}\text{Sr})_{\text{i}}$  ratios positively correlates with Sr, Ba, Rb and K<sub>2</sub>O contents, thus it could also be ascribed to participation of sediments in the source (e.g., Rehka and Hofman, 1997).

Plagiogranites show some significant variations in their isotopic ratios. Their initial Nd and Sr isotopic ratios tends to more radiogenic values  $+1.3 < \varepsilon_{\text{Nd}_{\text{I}}} < +5.5$ ;  $+5 < \varepsilon_{\text{Sr}_{\text{I}}} < +16$ , in agreement with significantly more radiogenic Pb and less radiogenic Hf isotopic ratios than the rest of the tholeiite series:  $(^{207}\text{Pb}/^{204}\text{Pb}) = 15.7$ ;  $(^{208}\text{Pb}/^{204}\text{Pb}) = 44.8$ ;  $(^{206}\text{Pb}/^{204}\text{Pb}) = 20.2$ ;  $\varepsilon_{\text{Hf}_{\text{I}}} = 5.6$ . These more radiogenic features correlate with a lower Nb/La ratio (in sample T-11-36), which is therefore in agreement with an increased subduction component.

To estimate the level of contamination which has occurred during the ophiolitic rocks formation, mixing curves have been

Bulk(1)= SI(43.70)AL(12.56)FE(13.69)MG(9.94)CA(11.70)TI(3.25)NA(3.15)K(0.20)O(163.545)H(60)O(30)

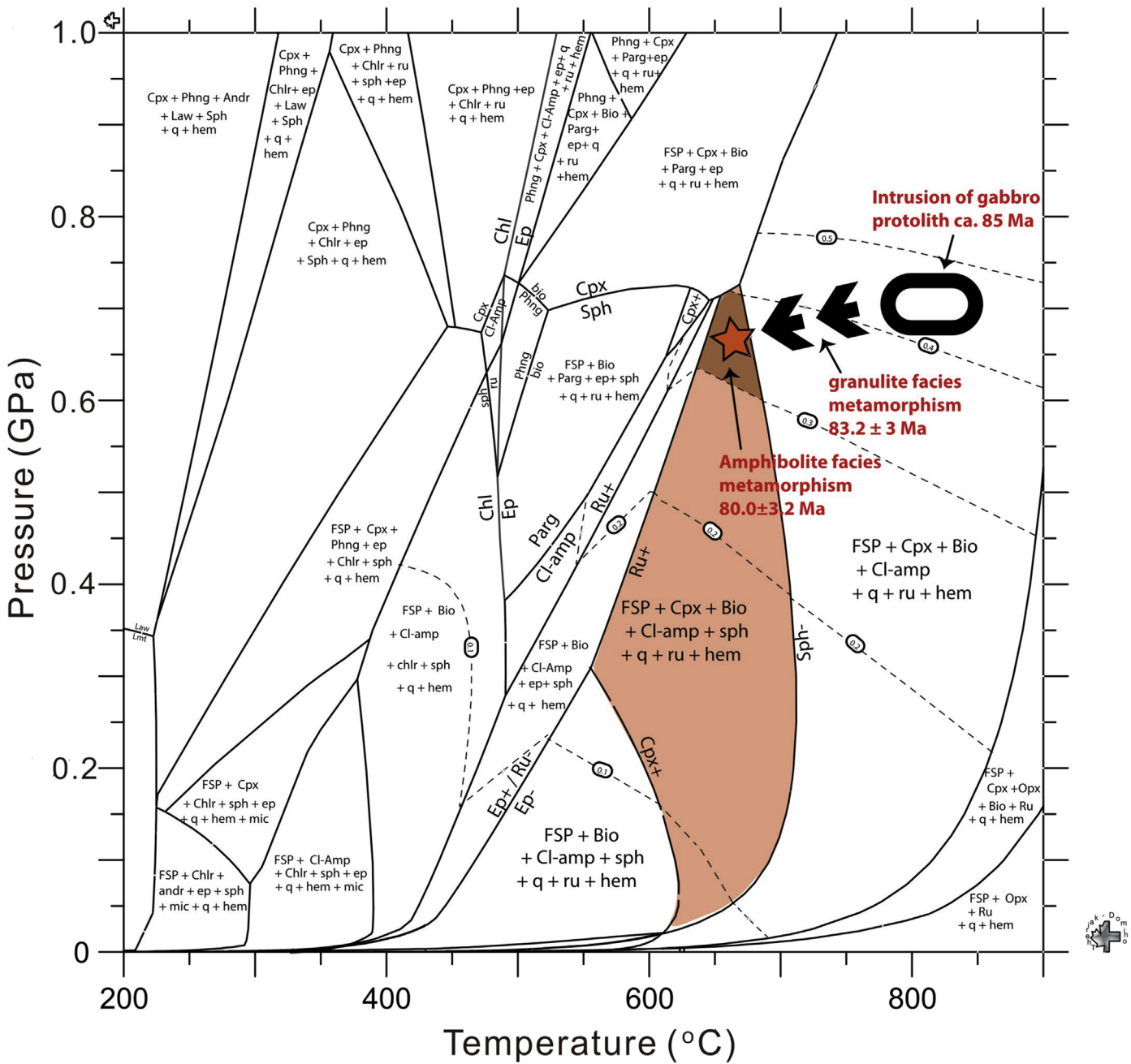


**Figure 12.** PT path of the Hinis amphibolites, from the Akdag HT unit. The equilibrium phase diagram was undertaken on the dated amphibolite sample T-11-30 using the software Theriaik-Domino (De Capitani and Petrakakis, 2010) in the  $\text{Na}_2\text{O}-\text{CaO}-\text{FeO}-\text{MgO}-\text{Al}_2\text{O}_3-\text{SiO}_2-\text{H}_2\text{O}-\text{TiO}_2-\text{O-H}$  (NCFMASHTOH) system. The internally consistent thermodynamic dataset of Holland and Powell (1998) and subsequent updates (tc55) were used. Mineral abbreviations are from Whitney and Evans (2010), for main phases see Fig. 10 caption.

drawn on Fig. 9H between different components: depleted mantle pole (MORB), Enriched Mantle 1 and Enriched Mantle 2 (EM1 and EM2, respectively; Zindler and Hart (1986), Salters and White (1998) and Hanan et al. (2000)). This isotopic modelling suggests that basaltic ophiolite lava composition results from contamination of a typical MORB by a possibly mixed source composed of EM1, EM2 and/or HIMU (Fig. 9H). Such contamination suggests the participation of subducted slab sediments in the source (EM1) and most likely a fertile E-MORB type source (EM2) or influence by seawater. Contamination by seawater is likely as highlighted by the spread towards higher  $\epsilon_{\text{Sr}}$  ratios than the

mantle correlation line in Fig. 9A. Plagiogranites show a more radiogenic source correlating with an increasing subduction affinity (Fig. 9D), but the high  $^{206}\text{Pb}/^{204}\text{Pb}$  ratios exclude to ascribe this trend to the sole effect of seawater alteration and sediment input. A possible mixing with a HIMU-type source is also suggested (Fig. 9H).

**3.1.2.2. Alkaline series.** Overall, alkaline lavas show, in comparison to ophiolite tholeiite rocks, lower initial  $\epsilon_{\text{Nd}_{\text{i}}}$  values ranging from +2.1 to +4.0 but have a similar range of  $(^{87}\text{Sr}/^{86}\text{Sr})_{\text{i}}$  ratios ( $-15 < \epsilon_{\text{Sr}_{\text{i}}} < +17$ ). In the  $\epsilon_{\text{Nd}_{\text{i}}}$  vs.  $\epsilon_{\text{Sr}_{\text{i}}}$  diagram (Fig. 9A) these rocks

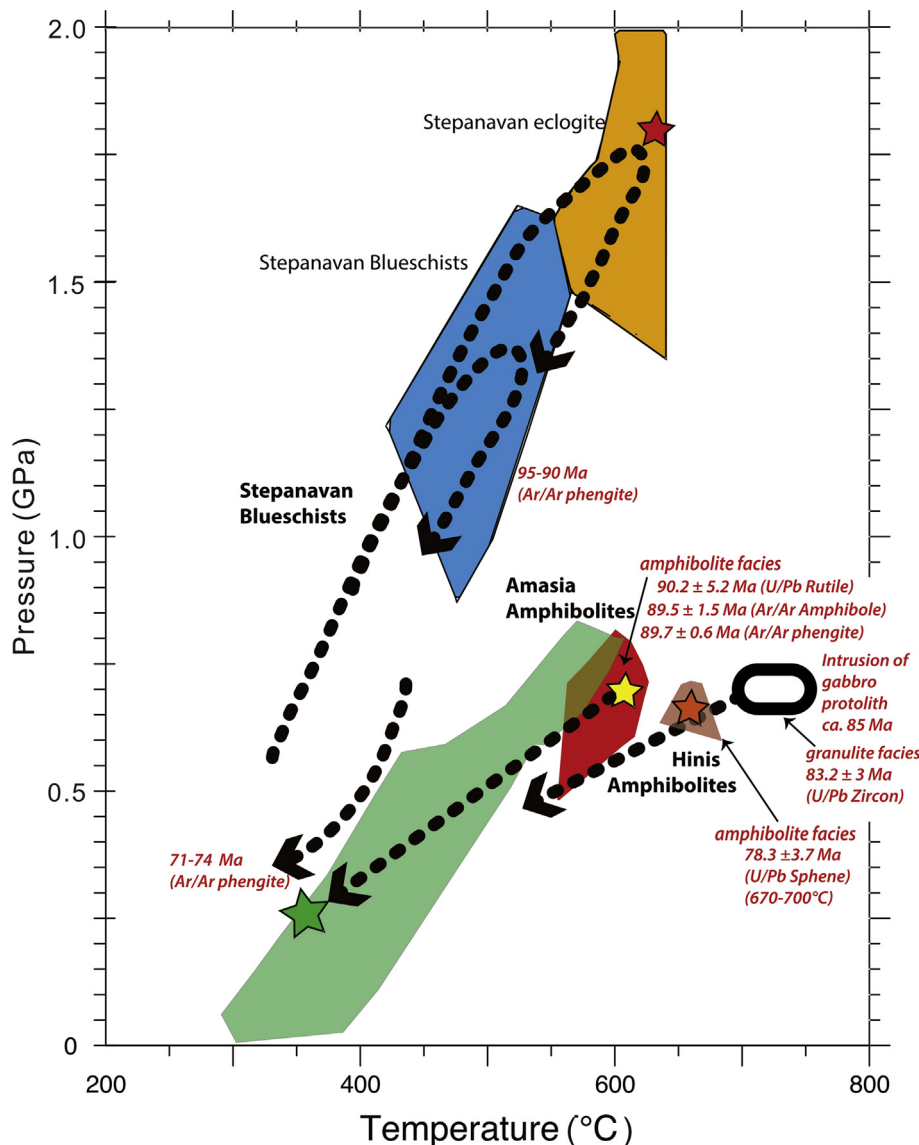


**Figure 13.** PT paths compiled from metamorphic rocks from units underthrusted by the non-metamorphic ophiolite. PT paths of Amasia and Stepanavan are after Hässig et al. (2019) and Rolland et al. (2009a).

are located in the OIB field. The lead isotopic ratios show higher values ( $^{207}\text{Pb}/^{204}\text{Pb}$ ) = 15.57–15.68; ( $^{208}\text{Pb}/^{204}\text{Pb}$ ) = 39.2–40.8; ( $^{206}\text{Pb}/^{204}\text{Pb}$ ) = 19.2–20.7 (Zindler and Hart, 1986), which are also in agreement with the contribution of a OIB source (Fig. 9E–H). In addition, the measured Hf isotopic ratios are the lowest of all analysed samples ( $\epsilon_{\text{Hf}} = 0.4$ –4.6, Fig. 9B), in agreement with OIB compositions (Fig. 9B). Isotopic modelling (Fig. 9H) suggests that the alkaline lava composition results from contamination of a typical MORB a more radiogenic source than EM2. HIMU, is the only contributor of lead with  $^{206}\text{Pb}/^{204}\text{Pb} > 19.2$  to the system, and is therefore invoked as a mixing component in many OIBs (e.g., Thirlwall, 1997; Bosch et al., 2014). Mixing curves suggest that composition results from the mixing of a MORB source with 7%–20% HIMU (Fig. 9H). However, spread in compositions in Fig. 9D–H shows that a combination of EM1–EM2 with HIMU is also required.

**3.1.2.3. Calc-alkaline series.** For the calc-alkaline lavas, the initial  $\epsilon_{\text{Nd}}$  values range from +2 to +6 and the  $\epsilon_{\text{Sr}}$  ratios range from

–15 to +17, respectively (Fig. 9A). The Pb and Hf isotopic ratios are slightly more radiogenic than those of the tholeiite suite rocks: ( $^{207}\text{Pb}/^{204}\text{Pb}$ ) = 15.58–15.67; ( $^{208}\text{Pb}/^{204}\text{Pb}$ ) = 38.7–39.0; ( $^{206}\text{Pb}/^{204}\text{Pb}$ ) = 18.6–18.9,  $\epsilon_{\text{Hf}} = 4.7$  (Fig. 9B–H). These values appear to be intermediate between those of ophiolitic tholeiites and alkaline rocks, and Sr isotopic ratios plot in the same range as these two series. Isotopic modelling (Fig. 9H) suggests that the calc-alkaline lava composition results from contamination of a typical MORB source by a significant amount of more radiogenic EM1–EM2 and HIMU sources, which reflects both the incorporation of a subduction component (Fig. 9C) and the contribution of mantle source similar to that of the alkaline series.

### 3.2. P-T-t conditions of the underthrusted TAP basement (Hinis, East Anatolia)

In this paper, we report new data on the TAP basement at Hinis (Fig. 3). For this study, we dated two samples by U/Pb dating of titanite. The samples are one amphibolite (sample T-11-30) and

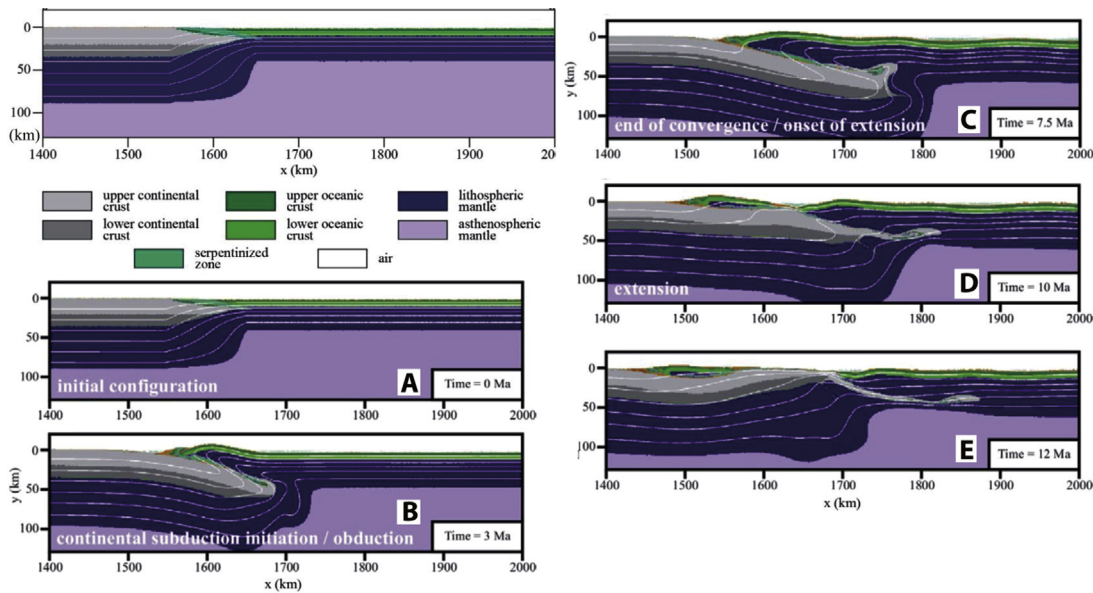


**Figure 14.** Numerical model of obduction (after Hässig et al., 2016a, b). The selected model encompasses an entirely thermally rejuvenated old oceanic lithosphere (80 Ma old lithosphere reheated during the Early Cretaceous plume events), with post-compression extension (5 cm/yr). For a full description of boundary conditions and details on the model used, the reader is referred to Hässig et al. (2016a, b). Top sketch: setup of the different layers in the model featuring the North Anatolia/SAB passive margin and OCT (Ocean-Continent Transition) with a serpentinized domain. Compressional and extensional velocities are applied at the lateral limits of the domain enlargement. The full model domain is a 4000 km × 1400 km box that includes asthenospheric mantle. Sketches A to E simulate a reactivation of compression on a previously passive North Anatolian margin, after reheating of the oceanic domain. As illustrated in this figure, obduction of the oceanic lithosphere occurs within 7.5 Ma, and is followed by collapse towards the North due to reactivation of the northern Neotethys subduction zone, which can be amplified by roll-back of the South Tethyan slab South to Anatolia. The exhumation of underthrusted continental domains in this extensional setting occurs in 4.5 Ma.

one of cross-cutting tourmaline-bearing leucogranite/quartz-monzonite (sample T-11-26). Both samples show homogeneous, unzoned titanite. Sample T-11-30 has patches of metamorphic subhedral/anhedral titanite, which recrystallized with amphibole (Hornblende, Suppl. Mat. 3) and plagioclase ( $An_{40}$ ), at the expense of a former clinopyroxene-rutile bearing assemblage (Fig. 10A–C). Sample T-11-26 leucogranite shows perfect euhedral titanite (Fig. 10D), which crystallized as an early magmatic phase, and occurs as inclusions within large K-feldspars.

The analytical procedures of U/Pb dating are displayed in Appendix A and the results are displayed on Appendix C Table and in Fig. 11. All sample T-11-30 individual spots grains are well aligned on a discordia line in the Tera-Wasserburg diagram, which defines a lower intercept age of  $80.0 \pm 3.2$  Ma ( $2\sigma$ ; MSWD = 0.31; Fig. 11). U/Pb dating on titanite of leucogranite sample T-11-26 yielded a well-defined lower intercept age of  $78.3 \pm 3.7$  Ma ( $2\sigma$ ; MSWD = 0.84; Fig. 11). These data are thus in good agreement with the previous datings of Topuz et al. (2017) on basement gneisses. The age of HT metamorphism obtained by two distinct methods (U/Pb on zircon in Topuz et al. (2017) and titanite in this study) is similar within error at  $\sim 80$  Ma. In addition, we show here that the cross-cutting leucogranites have, within errors, a similar age as the amphibolites. This is in agreement with a common origin, i.e. derivation of the leucogranites from the partial melting of basement metamorphic rocks.

Thermobarometry was undertaken on the dated amphibolite sample T-11-30. We computed the equilibrium phase diagram using the software Theria-Domino (De Capitani and Petrakakis, 2010) (Fig. 12). The internally consistent thermodynamic dataset of Holland and Powell (1998) and subsequent updates (tc55) were used. Equilibrium phase diagrams were calculated in the  $Na_2O-CaO-FeO-MgO-Al_2O_3-SiO_2-H_2O-TiO_2-OH$  (NCFMASH-TOH) system. The stability field of the peak metamorphic assemblage (Feldspar – Clinopyroxene – Biotite-Clino-Amphibole – Titanite – Quartz – Rutile – Hematite) lies between 550 °C and

710 °C and pressures between 0.05 GPa and 0.72 GPa. Based on the composition of amphibole ( $0.3 < Al^{VI} < 0.4$ , Suppl. Mat. 3) measured by EPMA and the corresponding isopleths computed from Theria-Domino, the stability field of T-11-30 amphibolite is estimated to be at  $660 \pm 20$  °C and  $0.66 \pm 0.06$  GPa. Accordingly, the thin section exhibits Hornblende + Clinopyroxene + Titanite + Plagioclase + Hematite (Fig. 10A–C). Towards the foliation planes, Clinopyroxene is totally replaced by Hornblende (Fig. 10A), and rutile inclusions occur within titanite, which suggest the main Amphibole-Titanite assemblage replaced a former Clinopyroxene-Rutile assemblage (Fig. 12). These mineralogical relationships agree for a P-T path coming from a higher temperature, granulite facies, domain ( $T > 700$  °C; Fig. 12).

#### 4. Discussion

The obduction process in the Anatolia-Armenia region is characterized by several first order geological constraints, which may be put forward to explain it. These include:

- The ophiolites in the studied regions represent remnants of a single ophiolite nappe currently of generally less than one to only a few kilometers thick. The nappe consists of an oceanic lithosphere older than 80 Ma at the time of its obduction, dominated by slightly serpentinized peridotites (e.g., Galoyan et al., 2009; Rolland et al., 2009b).
- The presence of widespread OIB-type magmatism preserved on top of the ophiolites is indicative of mantle upwelling processes (hotspot) active up to 5–10 Ma prior to obduction (e.g., Rolland et al., 2009b).
- Continental underthrusting of the TAP-SAB, evidenced in the crystalline basement rocks outcropping in the Hinis region (E Anatolia), and shows a metamorphic cycle compatible with a burial up to 0.66–0.8 GPa (20–25 km; Topuz et al., 2017), and

- rapid post-obduction core complex exhumation in less than 10 Ma.
- (iv) Between the TAP-SAB and the Pontides, an oceanic domain (~1000 km) remained to be subducted after the obduction, as evidenced by paleomagnetism on Coniacian-Santonian series (Meijers et al., 2015). In the following, we discuss on the main tectonic and magmatic phases, and on the triggering factors leading to this large-scale obduction.

#### 4.1. Significance of geochemical results for the origin, size and magmatic history of the East Anatolian-Armenian ophiolite nappe

On the basis of similar geochemical and radio chronological data concerning both ophiolitic and sub-ophiolitic lithologies as well as sedimentary records, the size of the reconstructed obducted ophiolitic nappe of the northern Neotethys segment (South of the Izmir-Ankara-Refahiye-Amasia-Sevan-Akera suture zone) is of at least 700 km in length and 100–200 km in width (Lordkipanidze et al., 1989; Rolland et al., 2011; Danelian et al., 2012; Hässig et al., 2013a,b, 2015, 2017) (Figs. 2, 4 and 5).

From West to East, a tendency is observed from fore-arc to back-arc sequence (Fig. 7).

The thick calc-alkaline domain underthrusted below the ophiolite at Erzincan exhibits a clear volcanic arc affinity, and should therefore correspond to the arc part of the obducted oceanic section. Its relatively low metamorphic conditions show that the volcanic arc sequence was not obducted by the whole ophiolite nappe, but was likely intercalated at intermediate depth within the nappe ( $P < 0.5$  GPa, Gücer and Aslan, 2014). As a whole, the underthrusted TAP-SAB margin suffered a low-grade metamorphic imprint, which is not clearly expressed in the carbonate rocks. Meijers et al. (2015) demonstrated that the paleomagnetic signal in the pre-obduction SAB limestones was fully reset during the obduction, which requires a temperature  $>200$  °C coherent with a burial below a 20 km ophiolite nappe.

#### 4.2. Time of obduction

The time for ophiolite obductions in the Middle East supports sub-coeval ophiolite obductions at c. 90–100 Ma in Anatolia (Parlak and Delaloye, 1999; Galoyan et al., 2009; Rolland et al., 2009b; Aslan et al., 2011; Hässig et al., 2013b, 2019; Plunder et al., 2016) and in Oman (95.5–96.5 Ma, e.g., Rioux et al., 2012) regions. The geochronological data synthesized in section 2 and the results of this paper converge to constrain a minimal age of about 95 Ma for intra-oceanic initiation of the obduction, highlighted by the HP rocks of the Stepanavan metamorphic unit (Figs. 5A and 13). Relatively similar (within error) ages of Erzincan meta-volcanic arc phyllites ( $100.8 \pm 3.4$  Ma to  $94.1 \pm 3.3$  Ma), suggest the incorporation of the volcanic arc within the obduction stack in the early stages of the nappe progression. Slightly younger ages obtained for the Amasia garnet amphibolites (91–88 Ma), in the obduction sole, argue for the propagation of the ophiolite in relatively hot conditions.

#### 4.3. Distance of ophiolite transport during obduction

Considering the distance between the suture zone and identified obduction fronts, in their present-day location, a minimum of 100 km of thrusting is needed to reach areas such as Vedi (Armenia) or Hinis (Turkey) and up to 200 km are necessary to reach Khoy (Iran) (Khalatbari-Jafari et al., 2004; Rolland et al., 2009a; Yilmaz and Yilmaz, 2013; Avagyan et al., 2017).

#### 4.4. Reasons for the obduction: numerical modelling

Given the ~80 Ma time span which separates the creation of oceanic lithosphere and the onset of the obduction of the ophiolitic nappe, the buoyancy of the cold oceanic lithosphere should lead to a simple subduction and not to obduction (Hässig et al., 2016a, b). The emplacement of an old (~80 Ma at the time of obduction) oceanic crust over large distances (up to 300 km) onto a continental crust is a puzzling geological problem. The main explanation for the transport of oceanic lithosphere onto the TAP-SAB is a net increase in oceanic lithosphere buoyancy, based on the finding of widespread hot-spot events in the North Neotethys domain leading to emplacement of the alkaline series throughout the Anatolian-Armenian ophiolite (Hässig et al., 2015, 2016a, b; Figs. 14 and 15). Numerical modelling based on a simplified Ocean-Continent Transition (OCT) allows to validate this hypothesis. As illustrated in Fig. 14, obduction of the oceanic lithosphere occurs within 7.5 Ma (Hässig et al., 2016a, b). The thinning of the obducted nappe is followed by collapse towards the North of oceanic lithosphere, due to reactivation of the northern Neotethys subduction zone, which would have been amplified by roll-back of the South Tethyan slab to the South of Anatolia. As shown by the modelling, the exhumation of underthrusted continental domains in this extensional setting occurs in 4.5 Ma (Hässig et al., 2016a, b).

#### 4.5. Post-obduction extensional thinning of the obducted nappe

In this paper (section 3), we obtain new constraints for the metamorphism and magmatism of the Anatolian-SAB blocks during and after the obduction, which give insights into the degree of continental underthrusting and the behaviour of the obducted oceanic lithosphere after its emplacement on top of the TAP-SAB continental crust. Thermobarometry undertaken on Hinis amphibolites yielded PT conditions of  $660 \pm 20$  °C and  $0.66 \pm 0.06$  GPa, while Topuz et al. (2017), who obtained ~0.7 GPa by conventional geobarometry, and slightly higher temperatures of 760–830 °C (by Ti-in-zircon and Zr-in-rutile thermometry). These pressure estimates agree for 20–25 km burial of these Paleozoic (Ordovician) meta-sedimentary units (Figs. 12 and 13). If we compare with geological sections of the Taurides, the thickness of sedimentary cover above the Ordovician would have reached a maximum of 3–4 km (Göncüoglu et al., 2004), thus ~20 km of burial can be ascribed to underthrusting below the ophiolite nappe (Fig. 15D). Dating of peak metamorphic conditions by Topuz et al. (2017) yielded an age of  $83.2 \pm 3$  Ma (U-Pb on zircon), which agrees with our U-Pb dating of titanite from amphibolites ( $80.0 \pm 3.2$  Ma). According to Scott and St-Onge (1995) and Pidgeon et al. (1996), the blocking temperature for titanite U/Pb dating is at 660–700 °C, which is similar/slightly above to the crystallization temperature obtained by thermobarometry, we thus assume that the obtained Titanite U/Pb age dates the time of metamorphic recrystallization in the amphibolite facies. The slight  $P-T-t$  difference obtained for granulites and amphibolites is ascribed to the fact that rutiles described by Topuz et al. (2017) are included within garnet cores, and the dated zircon comes from metapelites which underwent a significant migmatization. Hence, the rocks dated by Topuz et al. (2017) might reflect an earlier stage of metamorphism. Accordingly, the T-11-30 amphibolites might represent a deformed and recrystallized equivalent of a pristine stage of post-obduction magmatic activity. The gabbro intrusives are dated at ca. 85 Ma by Topuz et al. (2017). However, based on unpublished geochemical data, these authors rule out the possibility of amphibolites to be the deformed equivalent of their dated gabbros, as amphibolites display an anorogenic alkaline affinity, while the gabbros have an orogenic tholeiitic affinity. The metamorphic fabric is cross-cut by

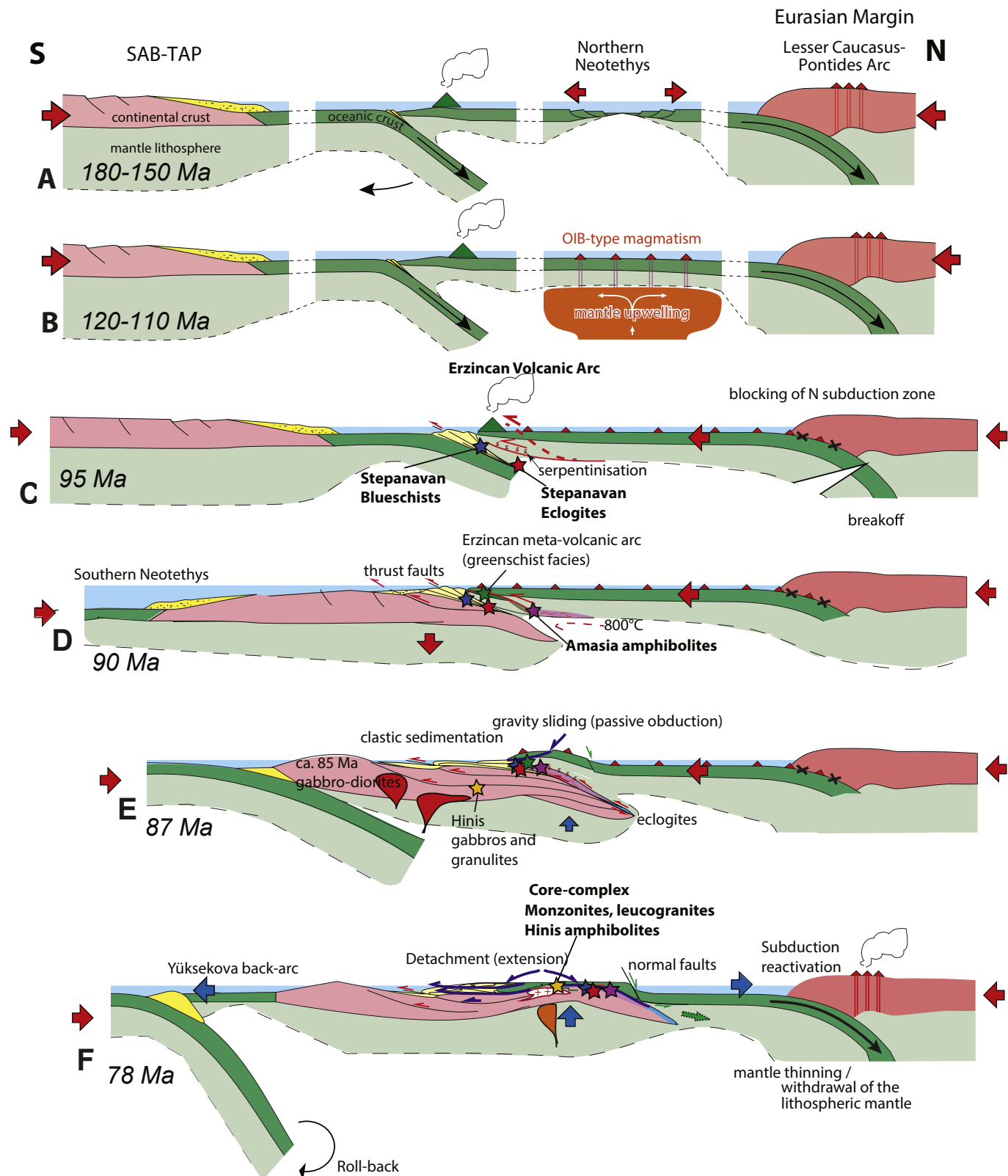


**Figure 15.** Sketch geodynamic model proposed for the formation and obduction of the oceanic lithosphere onto the northern margin of the Tauride-Anatolide Platform – South Armenian Block (TAP-SAB) from Early Jurassic to Late Cretaceous, combining field relationships, magmatic petrology, results from P-T paths and numerical modelling.

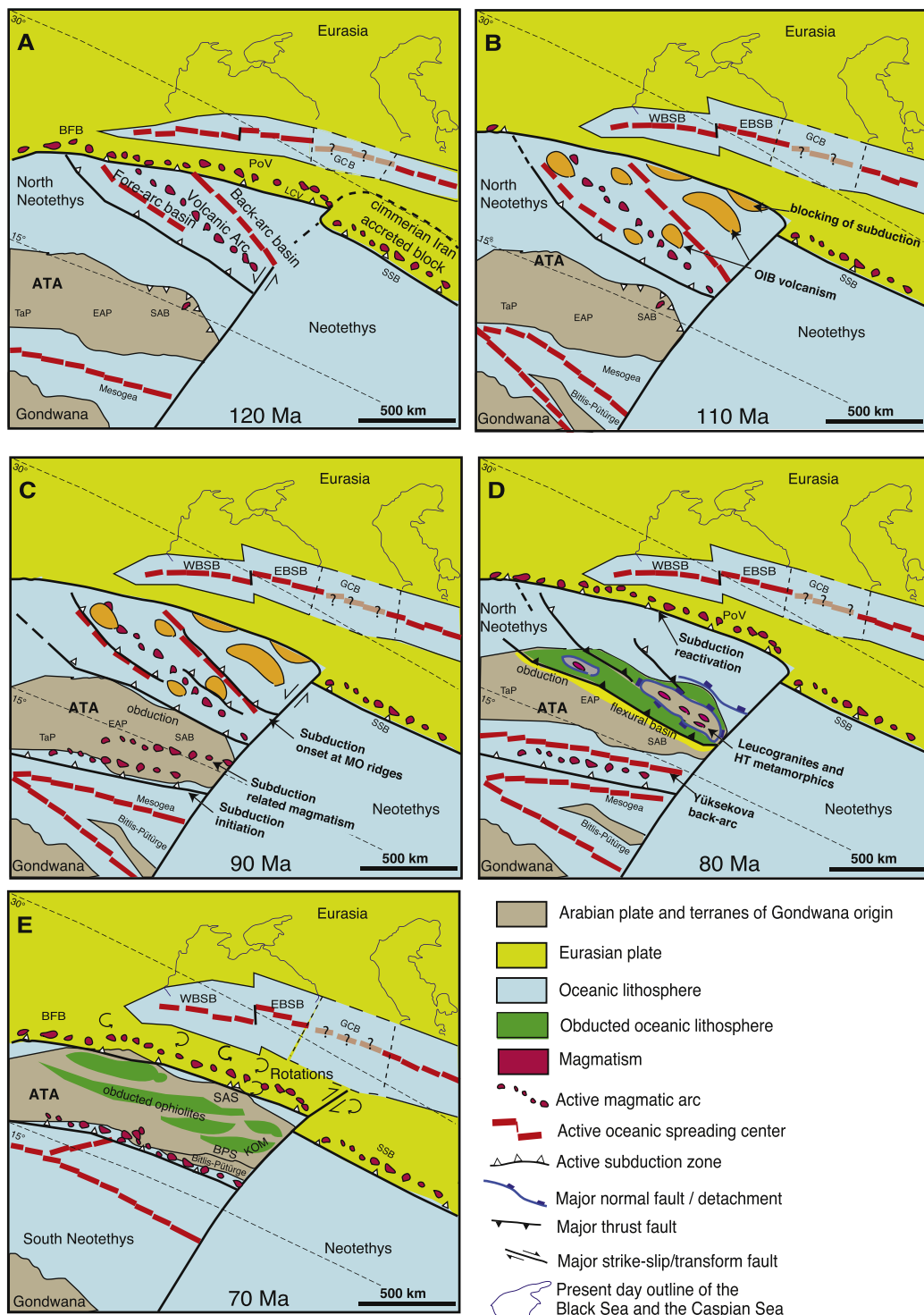


**Figure 16.** Palinspastic sketch reconstruction for Eastern Anatolia region, at the time of oceanic lithosphere obduction of the onto the northern margin of the TAP-SAB from Early to Late Cretaceous. Positions of blocks, oceans and general configuration are after Rolland (2017), modified from Barrier and Vrielynck (2008) and Moritz et al. (2016). ATA: Anatolites-Taurides block; ATB: Adjara-Trialeti basin; BFB: Balkan foldbelt; BPS: Bitlis-Pütürge suture; EAP: Eastern Anatolian platform; ECWIB: Eastern Caucasus Western Iran Boundary (or Araks Fault); EBSB: East Black Sea Basin; GCB: Greater Caucasus basin; KOM: Khojy ophiolite massif; LCR: Lesser Caucasus Range; LCV: Lesser Caucasus volcanic arc; MZT: Main Zagros thrust; NAF: North Anatolian Fault; PAM: Peri-Arabian massif; PoV: Pontides volcanic arc; PTB: Pontides-Transcaucasus block; SAB: South Armenian block; SAS: Sevan-Akera Suture; SCB: South-Caspian basin; SkB: Sakarya block; SSB: Sanandaj-Sirjan block; TaP: Taurus platform; Tc: Transcaucasus; WBSB: West Black Sea Basin. Question marks refer to the possible extension of the Great Caucasus basin, which closed in response to Arabia-Eurasia “soft” collision, as proposed by Cowgill et al. (2016) and Rolland (2017) and challenged by Vincent et al. (2017).

later leucogranites, which are dated at  $78.3 \pm 3.7$  Ma by U-Pb on titanite (this study). Consequently, the whole sequence of events, from gabbro emplacement to subsequent granulite and amphibolite metamorphic overprints, and their (greenschist facies)

overprint occurred within a short time range (85–78 Ma; Fig. 15E,F). The full exhumation of the metamorphic core happened before the Early Maastrichtian unconformity (ca. 70.6 Ma, after Yilmaz et al., 2010). Therefore, HP metamorphism and following

(20–23 km) exhumation necessitate high cooling (>80 °C/Myr) and uplift (>2 km/Myr to 2 mm/yr) rates from 85 Ma to 70 Ma. Based on the structural setting (highlighted in section 2.1.2 and Fig. 7), we suggest that the Hinis high grade rocks were exhumed below a nowadays flat tectonic contact overlain by an unmetamorphosed ophiolite (Topuz et al., 2017), and by the combination of steeper normal faults which branched down onto this flat contact (Fig. 15F). Such field relationships strongly suggest that the flat tectonic contact is a detachment, and not a thrust as previously proposed by Yilmaz et al. (2010). This major detachment structure exhumed the lower crust of Anatolia during the time constrained by the above *P-T-t* sequence. The detachment sustained activity during about 10 Ma is the best explanation for the high uplift rates and cooling rates deduced from the metamorphic study. As a matter of fact, onset of this major extensional phase onset occurred only 5 Ma after the obduction. Similar tectonic unroofing of metamorphic core complexes with detachment faulting during extensional collapse is also described in other obduction contexts such as Oman (Gray and Gregory, 2000; Fournier et al., 2006) and New Caledonia (e.g., Aitchison et al., 1995).

#### 4.6. Post-obduction extension and its relationship with subduction reactivation

What is the reason for this post-obduction extensional phase? Is it related somehow to subduction processes?

Several causes might be proposed: (1) extensional gravitational collapse due to instability of the superposition of an oceanic lithosphere above a continental lithosphere, triggered by the partial melting of the fluid-rich underthrusted continental crust (cf Vanderhaeghe, 2012) or by the delamination of the continental Lithosphere (Topuz et al., 2017), (2) back-arc extension following initiation of a subduction to the South of the TAP and roll-back of this subduction towards the south (Rolland et al., 2012), or (3) onset of a subduction zone in the northern Neotethys domain pulling back the obducted oceanic lithosphere towards the North (Hässig et al., 2015, 2017).

The fact that the East Anatolian metamorphism occurred during the intrusion of mantle-derived melts (gabbros, tonalites; Topuz et al., 2017) strongly suggests a subduction which was mature enough at 85 Ma (Fig. 15E). The timing of metamorphic and magmatic events along the SE Anatolian block is in good agreement with this hypothesis, as in Southern Anatolia, Karaoglan et al. (2016) obtained U-Pb zircon ages on subduction-related plutonic rocks ranging from 88 Ma to 81 Ma, with  $^{40}\text{Ar}/^{39}\text{Ar}$  ages indicating that these granitoids cooled below 300 °C in 6–10 Ma. Therefore, these authors give a confirmation for the activation of a subduction zone to the South of the Anatolian block by ca. 88 Ma, i.e., 2 Ma after the end of the obduction (Fig. 15D,E). Further, the age of the Yüksekovala ophiolite, which bounds to the South of the Anatolian block, preserves a back-arc affinity and is dated at  $81.9 \pm 0.6$  Ma to  $78.7 \pm 1$  Ma by  $^{40}\text{Ar}/^{39}\text{Ar}$  on hornblende (Rolland et al., 2012), confirmed by radiolarian dating by Tekin et al. (2015). Therefore, the Yüksekovala oceanic units, which have a back-arc basin affinity (Rolland et al., 2012; Ural et al., 2015) may have formed in response to roll-back of the South-Tethyan slab and marginal basin opening to the South of the Anatolian Block, as also proposed for SW Iran (Whitechurch et al., 2013). This phase of roll-back is a possible cause for the onset of post-obduction gravitational collapse. The extensional context in Anatolia-SAB may be also influenced by regained subduction below the Pontides-Transcaucasus margin (Fig. 15F). Finally, the age of the Bitlis HP rocks dates back to 70–74 Ma (Oberhänsli et al., 2010; Rolland et al., 2012). This suggests a phase of continent collision of the Bitlis terrane with Anatolia, which terminated the phase of Yüksekovala

back-arc basin opening and coincides with the end of extensional tectonics within the Anatolian plateau. To the North of the Neotethyan domain, post-obduction reactivation of subduction of the northern Neotethys domain occurs between early-middle Turonian and Santonian (84–90 Ma). This change of the northern Neotethys ocean boundary conditions is thus likely influential on the extensional tectonics leading to the tectonic thinning of the obducted ophiolite sequence (Fig. 15F). Therefore, the post-obduction tectonic collapse of the obducted ophiolite nappe is ascribed to a combination of processes including the thermal maturation of the underthrusted continental crust highlighted by the HT metamorphism of Hinis Akdag tectonic window, subduction and roll-back of the southern Neotethys slab to the South of Anatolia, and reactivation of subduction of the northern Neotethys slab below Pontides-Transcaucasus. The HT metamorphism of Hinis Akdag could result from a supra-subduction complex, or to the permanence of the hot-spot activity below the TAP.

#### 5. Conclusion

A model for the emplacement of the large-scale Anatolian-Armenian ophiolite is proposed on the base of the structural, geochemical and geochronological studies pertaining to preserved oceanic crust domains and of the metamorphic rocks beneath these ophiolites (Figs. 15 and 16):

- (1) The magmatic and ultrabasic rocks composing the ophiolitic nappe originate from a SSZ basin that slowly opened in a pre-existing ocean domain, while this domain subducted under Eurasia farther North (Figs. 15A and 16A). We thus infer the existence of an intra-oceanic subduction at this time (Early–Late Jurassic) and a probable roll-back of the intra-oceanic subduction slab as a motor for this spreading.
- (2) In the East Anatolian ophiolites, three magmatic suites are evidenced one on top of the other: (i) oceanic crust with tholeiitic magmatic rocks resembling N-MORB contaminated by slab fluids. This series is topped by (ii) basaltic flows or volcanic tuff with alkaline tendencies, which represent an OIB source, widespread in the northern Neotethys domain during the Early Cretaceous. Radiochronology and biostratigraphy both show that emplacement of this second suite occurs in an ocean environment prior to ophiolite obduction until Early–Late Cretaceous times. (iii) An Early/Late Cretaceous calc-alkaline series, with intermediate geochemical features between tholeiitic and alkaline is interpreted as resulting from the remelting product of a mantle previously contaminated by the OIB plume, in a supra-subduction zone context, at the onset of the obduction, in an intra-oceanic domain (Figs. 15B and 16B).
- (3) The Erzincan metavolcanics are suggested to represent the volcanic arc formed above the intra-oceanic subduction, which was further dragged under the obducting ophiolite through scaling, faulting and tectonic erosion (Fig. 15C,D).
- (4) Reconstructions of the ophiolitic nappe account for a length up to 2300 km of ophiolite overthrusting from the present suture zone to Khoy (Iran), hypothesized to represent the most distal obduction front (Fig. 16D). The olistostrome yields a lower chronological limit to this obduction to the Cenomanian (ca. 94 Ma). This observation is coherent with metamorphic ages for Erzincan low-grade metamorphic unit, the Amasia garnet amphibolites and the Stepanavan blueschists (Fig. 15C,D).
- (5) In order to explain such an obduction event, the oceanic crust thrusted in the proposed pre-obduction setup must be particularly hot. The heating of the oceanic lithosphere would be due to important upwelling mantle flows, evidenced by the alkaline

volcanism on the ophiolite, thus altering its rheological properties (Figs. 15B and 16C). This hypothesis is validated by a numerical model.

(6) Post-obduction gravitational collapse (Figs. 15E,F and 16D) is ascribed to a combination of (1) subduction and roll-back of the southern Neotethys slab to the South of Anatolia, (2) reactivation of subduction of the northern Neotethys slab below Pontides–Transcaucasus and (3) thermal maturation of the underthrusted Anatolian continental crust.

## Acknowledgements

This work was supported by the MEBE (Middle East Basin Evolution) and DARIUS programs jointly supported by a consortium including oil companies, UMPC and the INSU,CNRS. G. Topuz acknowledges TÜBİTAK grant (#114Y226) for support in field works. Y. Rolland acknowledges internal support of Geoazur for funding the master degree of R. Melis. Constructive remarks by two anonymous reviewers and the editor, Emilio Saccani, have helped to significantly improve the first version of the manuscript.

## Appendix A. Supplementary data

Supplementary data to this article can be found online at <https://doi.org/10.1016/j.gsf.2018.12.009>.

## References

- Abbate, E., Bortolotti, V., Passerini, P., Principi, G., 1985. The rhythm of Phanerozoic ophiolites. *Ophioliti* 10, 109–138.
- Abouchami, W., Goldstein, S.L., 1995. A lead isotopic study of Circum-Antarctic manganese nodules. *Geochimica et Cosmochimica Acta* 59, 1809–1820.
- Abovyan, S.B., 1981. The Mafic-Ultramafic Complexes of the Ophiolitic Zones in Armenian SSR. Izd. NAS Arm. SSR, 306 p. (in Russian).
- Adamia, S.A., Lordkipanidze, M.B., Zakariadze, G.S., 1977. Evolution of an active continental margin as exemplified by the Alpine history of the Caucasus. *Tectonophysics* 40, 183–189.
- Agard, P., Jolivet, L., Vrielynck, B., Burov, E., Monié, P., 2007. Plate acceleration: the obduction trigger? *Earth and Planetary Science Letters* 258, 428–441.
- Agard, P., Zuo, X., Funiciello, F., Bellahsen, N., Faccenna, C., Savva, D., 2014. Obduction: why, how and where, Clues from analog models. *Earth and Planetary Science Letters* 393, 132–145.
- Aitchison, J.C., Clarke, G.L., Meffre, S., Cluzel, D., 1995. Eocene arc-continent collision in New Caledonia and implications for regional southwest Pacific tectonic evolution. *Geology* 23 (2), 161–164.
- Arakelyan, R.A., 1964. The paleozoic-mesozoic. In: The Geology of the Armenian SSR: Stratigraphy. Publishing House of the AS of the Armenian SSR, Yerevan, pp. 21–163.
- Asatryan, G., Danelian, T., Sosson, M., Sahakyan, L., Person, A., Avagyan, A., Galoyan, G., 2010. Radiolarian ages of the sedimentary cover of Sevan ophiolite (Armenia, Lesser Caucasus). *Ophioliti* 35, 91–101.
- Asatryan, G., Danelian, T., Sosson, M., Sahakyan, L., Galoyan, G., 2011. Radiolarian evidence for Early Cretaceous (late Barremian – early Aptian) submarine volcanic activity in the Tethyan oceanic realm preserved in Karabagh (Lesser Caucasus). *Ophioliti* 36, 117–123.
- Asatryan, G., Danelian, T., Seyler, M., Sahakyan, L., et al., 2012. Latest Jurassic-Early Cretaceous radiolarian assemblages constrain episodes of submarine volcanic activity in the Tethyan oceanic realm of the Sevan ophiolites (Armenia). *Bulletin de la Societe Geologique de France* 183, 319–330.
- Aslan, Z., Gücer, M.A., Arslan, M., 2011.  $^{39}\text{Ar}$ - $^{40}\text{Ar}$  dating on plagioclases of metabasic metagranitic rocks in the Yoncayolu metamorphic, NE Turkey. *Goldschmidt Conference Abstracts* 460.
- Avagyan, A., Shahidi, A., Sosson, M., Sahakyan, L., Galoyan, G., Muller, C., et al., 2017. New data on the tectonic evolution of the Khoj region, NW Iran. *Geological Society, London, Special Publications* 428 (1), 99–116.
- Baghdasaryan, G.P., Ghukasyan, R.Kh., 1983. The age of Bjni migmatite-granitic massif (By the Rb-Sr isochrone radiometric data and geological ideas). *Proceedings NAS RA, Earth Sciences* 6, 15–29 (in Russian).
- Barrier, E., Vrielynck, B., 2008. Palaeotectonic Map of the Middle East, Atlas of 14 Maps, Tectono-sedimentary-Palinspastic Maps from Late Norian to Pliocene. Commission for the Geologic Map of the World. CCMW, CCGM, Paris.
- Bazhenov, M., Burtman, V.S., Levasheva, N.M., 1996. Lower and middle jurassic paleomagnetic results from the South lesser Caucasus and the evolution of the mesozoic tethys ocean. *Earth and Planetary Science Letters* 141, 79–89.
- Biju-Duval, B., Dercourt, J., Le Pichon, X., 1977. From the tethys ocean to the Mediterranean seas: a plate tectonic model of the evolution of the western alpine system. In: Biju-Duval, B., Montadert, L. (Eds.), *Structural History of the Mediterranean Basins*. Editions Technip, Paris, pp. 143–164.
- Bortolotti, V., Chiari, M., Goencueoglu, M.C., Principi, G., Saccani, E., Tekin, U.K., Tassinari, R., 2018. The Jurassic–Early Cretaceous basalt–chert association in the ophiolites of the Ankara Mélange, east of Ankara, Turkey: age and geochemistry. *Geological Magazine* 155 (2), 451–478.
- Bosch, D., Jamais, M., Boudier, F., Nicolas, A., Dautria, J.M., Agrinier, P., 2004. Deep and high temperature hydrothermal circulation in the Oman ophiolite. Petrological and isotopic evidence. *Journal of Petrology* 45, 1181–1203.
- Bosch, D., Maury, R.C., El Azzouzi, M., Bollinger, C., Bellon, H., Verdoux, P., 2014. Lithospheric origin for Neogene–quaternary middle Atlas lavas (Morocco): clues from trace elements and Sr–Nd–Pb–Hf isotopes. *Lithos* 205, 247–265.
- Boudier, F., Ceuleneer, G., Nicolas, A., 1988. Shear zones, thrusts and related magmatism in the Oman ophiolite: initiation of thrusting on an oceanic ridge. *Tectonophysics* 151, 275–296.
- Bozkurt, E., Mittwede, S.K., 2001. Introduction to the geology of Turkey – a synthesis. *International Geology Review* 43, 578–594.
- Bozkuş, C., 1998. Stratigraphy and structural evolution of Pontid/Anatolid suture zone in NE Anatolia (between Oltu-Narman). *Journal of Engineering Science* 4, 487–499.
- Cannat, M., 1993. Emplacement of mantle rocks in the seafloor at mid-ocean ridges. *Journal of Geophysical Research: Solid Earth* 98 (B3), 4163–4172.
- Çelik, Ö.F., Delaloye, M., Feraud, G., 2006. Precise  $^{40}\text{Ar}$ / $^{39}\text{Ar}$  ages from the metamorphic sole rocks of the Tauride Belt ophiolites, southern Turkey: implications for the rapid cooling history. *Geological Magazine* 143, 213–227.
- Çelik, Ö.F., Marzoli, A., Marschik, R., Chiaradia, M., Neubauer, F., Öz, I., 2011. Early–middle jurassic intra-oceanic subduction in the Izmir-Ankara-Erzincan ocean, northern Turkey. *Tectonophysics* 509, 120–134.
- Chan, G.H.N., Malpas, J., Xenophontos, C., Lo, C.H., 2007. Timing of subduction zone metamorphism during the formation and emplacement of Troodos and Baer-Bassit ophiolites: insights from  $^{40}\text{Ar}$ / $^{39}\text{Ar}$  geochronology. *Geological Magazine* 144, 797–810.
- Çimen, O., Göncüoğlu, M.C., Simonetti, A., Sayit, K., 2018. New zircon U-Pb LA-ICP-MS ages and Hf isotope data from the Central Pontides (Turkey): geological and geodynamic constraints. *Journal of Geodynamics* 116, 23–36.
- Cloos, M., Shreve, R.L., 1988. Subduction-channel model of prism accretion, melange formation, sediment subduction, and subduction erosion at convergent plate margins: 1. Background and description. *Physical Applied Geophysics* 128, 456–500.
- Coleman, R.G., 1971. Plate tectonic emplacement of upper mantle peridotites along continental edges. *Journal of Geophysical Research* 76, 1212–1222.
- Coleman, R.G., 1981. Tectonic setting for ophiolite obduction in Oman. *Journal of Geophysical Research* 86, 2497–2508.
- Cowgill, E., Forte, A.M., Niemi, N., Avdeev, B., Tye, A., Trexler, C., ..., Godoladze, T., 2016. Relict basin closure and crustal shortening budgets during continental collision: An example from Caucasus sediment provenance. *Tectonics* 35 (12), 2918–2947.
- Danelian, T., Galoyan, G., Rolland, Y., Sosson, M., 2007. Palaeontological (radiolarian) late jurassic age constraint for the Stepanavan ophiolite (Lesser Caucasus, Armenia). *Bulletin of the Geological Society of Greece* 40, 31–38.
- Danelian, T., Asatryan, G., Sosson, M., Person, A., Sahakyan, L., Galoyan, G., 2008. Discovery of middle jurassic (Bajocian) radiolaria from the sedimentary cover of the Vedi ophiolite (Lesser Caucasus, Armenia). *Comptes Rendus Pal Evol* 7, 327–334.
- Danelian, T., Asatryan, G., Sahakyan, L., Galoyan, G., Sosson, M., Avagyan, A., 2010. New and revised radiolarian biochronology for the sedimentary cover of ophiolites in the Lesser Caucasus (Armenia). *Geological Society, London, Special Publications* 340, 383–391.
- Danelian, T., Asatryan, G., Galoyan, G., Sosson, M., Sahakyan, L., Caridroit, M., Avagyan, A., 2012. Geological history of ophiolites in the Lesser Caucasus and correlation with the Izmir-Ankara-Erzincan suture zone: insights from radiolarian biochronology. *Bulletin de la Societe Geologique de France* 183, 331–342.
- Danelian, T., Zambetakis-Lekkas, A., Galoyan, G., Sosson, M., Asatryan, G., Hubert, B., Grigiryan, A., 2014. Reconstructing Upper Cretaceous (Cenomanian) paleo environments in Armenia based on radiolarian and benthic foraminifera; implications for the geodynamic evolution of the Tethyan realm in the Lesser Caucasus. *Palaeogeography, Palaeoclimatology, Palaeoecology* 413, 123–132.
- Dercourt, J., Zonenschain, L.P., Ricou, L.-E., Kazmin, V.G., et al., 1986. Geological evolution of the Tethys belt from the Atlantic to the Pamirs since the Lias. *Tectonophysics* 123, 241–315.
- Dewey, J.F., Bird, J.M., 1971. Origin and emplacement of the ophiolite suite: Appalachian ophiolites in Newfoundland. *Journal of Geophysical Research* 76, 3179–3206.
- Dewey, J.F., 1976. Ophiolite obduction. *Tectonophysics* 31, 93–120.
- De Capitani, C., Petrakakis, K., 2010. The computation of equilibrium assemblage diagrams with Theria/Domino software. *American Mineralogist* 95 (7), 1006–1016.
- Dilek, Y., Whitney, D.L., 1997. Counterclockwise PT trajectory from the metamorphic sole of a Neo-Tethyan ophiolite (Turkey). *Tectonophysics* 280, 295–310.
- Dilek, Y., Thy, P., Hacker, B., Grundvig, S., 1999. Structure and petrology of Tauride ophiolites and mafic dike intrusions (Turkey): implications for the Neotethyan ocean. *Geological Society of America Bulletin* 111, 1192–1216.

- Dimo-Lahitte, A., Monié, P., Vergély, P., 2001. Metamorphic soles from the Albanian ophiolites: petrology,  $^{40}\text{Ar}/^{39}\text{Ar}$  geochronology, and geodynamic evolution. *Tectonics* 20, 78–96.
- Dokuz, A., Aydin, F., Karslı, O., 2019. Post-collisional transition from subduction- to intraplate-type magmatism in the eastern Sakarya Zone, Turkey: Indicators of the northern Neotethyan slab breakoff. *Geological Society of America Bulletin*. <https://doi.org/10.1130/B31993.1>.
- Duretz, T., Agard, P., Yamato, P., Ducassou, C., Burov, E.B., Gerya, T.V., 2016. Thermo-mechanical modeling of the obduction process based on the Oman ophiolite case. *Gondwana Research* 32, 1–10.
- Elitok, Ö., Drüppel, K., 2008. Geochemistry and tectonic significance of metamorphic sole rocks beneath the Beyoehir–Hoyran ophiolite (SW-Turkey). *Lithos* 100, 322–353.
- Evensen, N.M., Hamilton, P.J., O’Nions, R.K., 1978. Rare earth abundances in chondritic meteorites. *Geochimica et Cosmochimica Acta* 42, 1199–1212.
- Festa, A., Pini, G.A., Dilek, Y., Codegone, G., 2010. Mélanges and mélange-forming processes: a historical overview and new concepts. *International Geology Review* 52, 1040–1105.
- Fournier, M., Leprvier, C., Razin, P., Jolivet, L., 2006. Late cretaceous to paleogene post-obduction extension and subsequent Neogene compression in Oman mountains. *GeoArabia* 11, 17–40.
- Galoyan, Gh., 2008. Petrologic, Geochemical and Geochronological Studies of the Ophiolites of the Lesser Caucasus (Armenia) (PhD thesis). University of Nice-Sophia Antipolis, 287p. (in French).
- Galoyan, G., Rolland, Y., Sosson, M., Corsini, M., Melkonyan, R., 2007. Evidence for superposed MORB, oceanic plateau and volcanic arc series in the Lesser Caucasus (Stepanavan, Armenia). *Comptes Rendus Geoscience* 339, 482–492.
- Galoyan, G., Rolland, Y., Sosson, M., Corsini, M., Billo, S., Verati, C., Melkonyan, R., 2009. Geology, geochemistry and  $^{40}\text{Ar}/^{39}\text{Ar}$  dating of sevan ophiolites (lesser Caucasus, Armenia): evidence for jurassic back-arc opening and hot spot event between the south Armenian block and Eurasia. *Journal of Asian Earth Sciences* 34, 135–153.
- Galoyan, Gh., Melkonyan, R.L., Chung, S.-L., Khorenyan, R.H., Atayan, L.S., Hung, C.-H., Amiraghyan, S.V., 2013. To the petrology and geochemistry of jurassic island-arc magmatics of the Karabagh segment of the Somkheto-Karabagh terrain. *Proceedings NAS RA, Earth Sciences* 66 (1), 3–22 (in Russian).
- Galoyan, Gh., Melkonyan, R., Chung, S.L., Khorenyan, R.H., Lee, Y.H., Amiraghyan, S.V., 2018. On the petrology and geochemistry of jurassic magmatics of the Somkheto segment of Somkheto-Karabagh tectonic zone (northern Armenia). *Proceedings NAS of Armenia, Earth Sciences* 1 (in press).
- Gealey, W.K., 1988. Plate tectonic evolution of the Mediterranean-Middle East region. *Tectonophysics* 155, 285–306.
- Gedik, A., 2008. Geology of the Tertiary rocks around Kemah-Erzincan-Çayırı region and their source rock characteristics. *Türkiye Mineral Resource Exploration Bulletin* 137, 1–27.
- Ghazaryan, H.A., 1994. Peculiarities of the geological structures and petrogenesis of ophiolitic gabbroids, on the examples of the Sevan and Vedi ophiolite zones of Armenia. *Izvestia NAS of Armenia, Nauki o Zemle* 3, 19–31 (in Russian).
- Göncüoğlu, M.C., 2010. Introduction to the Geology of Turkey: Geodynamic Evolution of the Pre-Alpine and Alpine Terranes.
- Göncüoğlu, M.C., Tekin, U.K., Turhan, N., 2001. Late Carnian radiolarite-bearing basalt blocks within the Late Cretaceous central Sakarya ophiolitic mélange, NW Anatolia: geological constraints. In: Proceedings of the 54th Geological Congress of Turkey, CD-Format. Chamber of Geological Engineering of Turkey, pp. 54–61.
- Göncüoğlu, M.C., Göncüoğlu, Y., Kozlu, H., Kozur, H.W., 2004. Geological evolution of the Taurides during the Infra-Cambrian to Carboniferous period: a Gondwanan perspective based on new biostratigraphic findings. *Geologica Carpathica* 55 (6), 433–447.
- Göncüoğlu, M.C., Yalınçın, M.K., Tekin, U.K., 2006. Geochemistry, tectono-magmatic discrimination and radiolarian ages of basic extrusives within the Izmir-Ankara suture belt (NW Turkey): time constraints for the Neotethyan evolution. *Ophioliti* 31, 25–38.
- Gray, D.R., Gregory, R.T., 2000. Implications of the structure of the Wadi Tayin metamorphic sole, the Ibra-Dasir block of the Samail ophiolite, and the Saïh Hatat window for late stage extensional ophiolite emplacement, Oman. *Marine Geophysical Research* 21 (3–4), 211–227.
- Güler, M.A., Aslan, Z., Bektas, O., 2007. Petrography and geochemistry features of the Yoncayolu metamorphics in Erzincan, NE Turkey. *Glodschmidt Conference Abstracts* A360.
- Güler, M.A., Aslan, Z., 2014.  $^{40}\text{Ar}/^{39}\text{Ar}$  age, petrography and geochemistry of the Yoncayolu metamorphic rocks (NE Turkey): subduction-related metamorphism under greenschist facies conditions. *Neues Jahrbuch für Mineralogie-Abhandlungen. Journal of Mineralogy and Geochemistry* 191 (3), 257–276.
- Hanan, B.B., Blachert-Toft, J., Kingsley, R., Schilling, J.G., 2000. Depleted Iceland mantle plume geochemical signature: artifact of multicomponent mixing? *Geochemistry, Geophysics, Geosystems* 1 (4). <https://doi.org/10.1029/1999GC000009>.
- Harris, N.B., Kelley, S., Okay, A.I., 1994. Post-collision magmatism and tectonics in northwest Anatolia. Contribution to Mineralogy and Petrology 117, 241–252.
- Hart, S.R., 1984. A large-scale isotope anomaly in the Southern Hemisphere mantle. *Nature* 309, 753–757.
- Hässig, M., Rolland, Y., Sosson, M., Galoyan, G., Müller, C., Avagyan, A., Sahakyan, L., 2013a. New structural and petrological data on the Amasia ophiolites (NW Sevan-Akera suture zone, Lesser Caucasus): insights for a large-scale obduction in Armenia and NE Turkey. *Tectonophysics* 588, 135–153.
- Hässig, M., Rolland, Y., Sosson, M., Galoyan, G., Sahakyan, L., Topuz, G., Çelik, Ö.F., Avagyan, A., Müller, C., 2013b. Linking the NE Anatolian and Lesser Caucasus ophiolites: evidence for large scale obduction of oceanic crust and implications for the formation of the Lesser Caucasus-Pontides Arc. *Geodinamica Acta* 26, 311–330.
- Hässig, M., Rolland, Y., Sahakyan, L., Sosson, M., Galoyan, G., Avagyan, A., Bosch, D., Müller, C., 2015. Multi-stage metamorphism in the South Armenian block during the Late Jurassic to early cretaceous: tectonics over south-dipping subduction of Northern branch of Neotethys. *Journal of Asian Earth Sciences* 102, 4–23.
- Hässig, M., Rolland, Y., Duretz, T., Sosson, M., 2016a. Obduction triggered by regional heating during plate reorganization. *Terra Nova* 28 (1), 76–82.
- Hässig, M., Duretz, T., Rolland, Y., Sosson, M., 2016b. Obduction of old oceanic lithosphere due to reheating and plate reorganization: insights from numerical modelling and the NE Anatolia–Lesser Caucasus case example. *Journal of Geodynamics* 96, 35–49.
- Hässig, M., Rolland, Y., Sosson, M., 2017. From seafloor spreading to obduction: jurassic–Cretaceous evolution of the northern branch of the Neotethys in the Northeastern Anatolian and Lesser Caucasus regions. *Geological Society, London, Special Publications* 428. <https://doi.org/10.1144/SP428.10>.
- Hässig, M., Rolland, Y., Melis, R., Sosson, M., Galoyan, G., Bruguier, O., 2019. P-T-t history of the Amasia and Stepanavan sub-ophiolitic metamorphic units (NW Armenia, Lesser Caucasus): implications for metamorphic sole development and for the obduction process. *Ophioliti* 44 (1), 43–70.
- Hatzipanagiotou, K., Pe-Piper, G., 1995. Ophiolitic and sub-ophiolitic metamorphic rocks of the Vatera area, southern Lesbos (Greece): geochemistry and geochronology. *Ophioliti* 20, 17–29.
- Hess, J.C., Aretz, J., Gurbani, A.G., Emmermann, R., Lippolt, H.J., 1995. Subduction related jurassic andesites in the northern Great Caucasus. *Geologische Rundschau* 84, 319–333.
- Holland, T.J.B., Powell, R.T.J.B., 1998. An internally consistent thermodynamic data set for phases of petrological interest. *Journal of Metamorphic Geology* 16 (3), 309–343.
- Huene, R., Ranero, C.R., Vannucchi, P., 2004. Generic model of subduction erosion. *Geology* 32, 913–916.
- Karaoglu, F., Parlak, O., Hejl, E., Neubauer, F., Klötzli, U., 2016. The temporal evolution of the active margin along the Southeast Anatolian Orogenic Belt (SE Turkey): evidence from U–Pb, Ar–Ar and fission track chronology. *Gondwana Research* 33, 190–208.
- Kazmin, V.G., 1991. Collision and rifting in the Tethys ocean: geodynamic implication. *Tectonophysics* 196, 371–384.
- Kawahata, H., Nohara, M., Ishizuka, H., Hasebe, S., Chiba, H., 2001. Sr isotope geochemistry and hydrothermal alteration of the Oman ophiolite. *Journal of Geophysical Research* 106 (B6), 11083–11099.
- Kergaravat, C., Ribes, C., Legeay, E., Callot, J.P., Kavak, K.S., Ringenbach, J.C., 2016. Minibasins and salt canopy in foreland fold-and-thrust belts: the central Sivas Basin, Turkey. *Tectonics* 35 (6), 1342–1366.
- Khalatbari-Jafari, M., Juteau, T., Bellon, H., Whitechurch, H., Cotten, J., Emami, H., 2004. New geological, geochronological and geochemical investigations on the Khoy ophiolites and related formations, NW Iran. *Journal of Asian Earth Sciences* 23, 507–535.
- Knipper, A.L., 1975. The oceanic crust in the structure of the alpine folded belt (south Europe, western part of Asia and Cuba). *Tr. GIN NAS USSR* 267, 207 (in Russian).
- Knipper, A.L., Khain, E.V., 1980. Structural position of ophiolites of the Caucasus. *Ophioliti*, Special Issue 2, 297–314.
- Koepke, J., Seidel, E., Kreuer, H., 2002. Ophiolites on the southern Aegean islands Crete, Karpathos and Rhodes: composition, geochronology and position within the ophiolite belts of the eastern Mediterranean. *Lithos* 65, 183–203.
- Koglin, N., 2008. Geochemistry, Petrogenesis and Tectonic Setting of Ophiolites and Mafic-Ultramafic Complexes in the Northeastern Aegean Region: New Trace-Elements, Isotopic and Age Constraints (Ph.D. thesis). Gutenberg University, Mainz, Germany, 136 p.
- Lagabielle, Y., 2009. Mantle exhumation and lithospheric spreading: an historical perspective from investigations in the Oceans and in the Alps–Apennines ophiolites. *Italian Journal of Geoscience (Bollettino Società Geologica Italiana)*, Sezione Tematica su Alps and Apennines 128, 279–293.
- Lagabielle, Y., Chauvet, A., Ulrich, M., Guillot, S., 2013. Passive obduction and gravity-driven emplacement of large ophiolitic sheets: the New Caledonia ophiolite (SW Pacific) as a case study? *Bulletin de la Société Géologique de France* 184 (6), 545–556.
- Lamphere, M.A., Coleman, R.G., Karamata, S., Pamiae, J., 1975. Age of amphibolites associated with Alpine peridotites in the Dinaride ophiolite zone, Yugoslavia. *Earth and Planetary Science Letters* 26, 271–276.
- Leroy, M., Dautueil, O., Cobbold, P.R., 2004. Incipient shortening of a passive margin: the mechanical roles of continental and oceanic lithospheres. *Geophysical Journal International* 159, 400–411.
- Lordkipanidze, M.B., Meliksetian, B., Djabarashian, R., 1989. Mesozoic-cenozoic magmatic evolution of the pontian–Crimean–Caucasian region. In: Rakús, M., Dercourt, J., Laird, A.E.M. (Eds.), *IGCP Project no. 198: Evolution of the Northern Margin of Tethys*, vol. 154. Mémoires de la Société Géologique de France, pp. 103–124.

- Maffione, M., Hinsbergen, D.J., 2018. Reconstructing plate boundaries in the jurassic Neo-Tethys from the east and west Vardar ophiolites (Greece, Serbia). *Tectonics*. <https://doi.org/10.1002/2017TC004790>.
- Marroni, M., Frassi, C., Göncüoğlu, M.C., Di Vincenzo, G., Pandolfi, L., Rebay, G., et al., 2014. Late jurassic amphibolite-facies metamorphism in the intra-pontide suture zone (Turkey): an eastward extension of the Vardar ocean from the Balkans into Anatolia? *Journal of the Geological Society* 171 (5), 605–608.
- Mart, Y., 1987. Superpositional tectonic patterns along the continental margin of the southeastern Mediterranean: a review. *Tectonophysics* 140, 213–232.
- Mattauer, M., Faure, M., Malavieille, J., 1981. Transverse lineation and large-scale structures related to Alpine obduction in Corsica. *Journal of Structural Geology* 3, 401–409.
- McCulloch, M.T., Gregory, R.T., Wasserburg, G.J., Taylor, J., 1981. Sm-Nd, Rb-Sr, and  $^{18}\text{O}/^{16}\text{O}$  systematics in an oceanic crustal section: evidence from the Samail ophiolite. *Journal of Geophysical Research* 86, 2721–2736.
- Meijers, M.J.M., Vrouwe, B., van Hinsbergen, D.J.J., Kuiper, K.F., Wijbrans, J., Davies, G.R., Kaymakçı, N., Matenco, L., Saintot, A., 2010. Jurassic arc volcanism on Crimea (Ukraine): implications for the paleo-subduction zone configuration of the Black Sea region. *Lithos* 119, 412–426.
- Meijers, M.J.M., Smith, B., Kirscher, U., Mensink, M., Sosson, M., Rolland, Y., Grigoryan, A., Sahakyan, L., Avagyan, A., Langereis, C., Müller, C., 2015. A paleolatitude reconstruction of the south Armenian block (Lesser Caucasus) for the late cretaceous: constraints on the Tethyan realm. *Tectonophysics* 644–645, 197–219.
- Meijers, M.J., Smith, B., Pastor-Galán, D., Degenar, R., Sadradze, N., Adamia, S., Sahakyan, L., Avagyan, A., Sosson, M., Rolland, Y., Langereis, C.G., Müller, C., 2017. Progressive orocline formation in the eastern pontides-lesser Caucasus. *Geological Society London Special Publications* 428. SP428–8.
- Moix, P., Beccaletto, L., Kozur, H.W., Hochard, C., Rossetted, F., Stampfli, G.M., 2008. A new classification of the Turkish terranes and sutures and its implication for the paleotectonic history of the region. *Tectonophysics* 451, 7–39.
- Monié, P., Agard, P., 2009. Coeval blueschist exhumation along thousands of kilometers: implications for subduction channel processes. *Geochemistry, Geophysics, Geosystems* 10, Q07002.
- Monin, A.S., Zonenshain, L.P., 1987. History of the Ocean Tethys. Moscow Institute of Oceanology (in Russian).
- Moores, E.M., 1982. Origin and emplacement of ophiolites. *Reviews of Geophysics* 20, 735–760.
- Moritz, R., Melkonyan, R., Selby, D., Popkhadze, N., Gugushvili, V., Tayan, R., Ramazanov, V., 2016. Metallogeny of the Lesser Caucasus: from arc construction to post-collision evolution. In: *Special Publications of the Society of Economic Geologists*, vol. 19, pp. 157–192.
- Mutter, J.C., Karson, J.A., 1992. Structural processes at slow-spreading ridges. *Science* 257, 627–634.
- Nikishin, A.M., Khotylev, A.O., Bychkov, A.Y., Kopaeich, L.F., Petrov, E.I., Yapaskurt, V.O., 2013. Cretaceous volcanic belts and the evolution of the Black Sea basin. *Moscow University Geology Bulletin* 68, 141–154.
- Oberhänsli, R., Candan, O., Bousquet, R., Rimmele, G., Okay, A., Goff, J., 2010. Alpine high pressure evolution of the eastern Bitlis complex, SE Turkey. *Geological Society, London, Special Publications* 340 (1), 461–483.
- Okay, A.Y., Şahintürk, Ö., 1997. Geology of the eastern Pontides. In: Robinson, A.G. (Ed.), *Regional and Petroleum Geology of the Black Sea and Surrounding Region*: American Association of Petroleum, vol. 68. *Geologists Memoir*, pp. 291–311.
- Okay, A.I., Nikishin, A.M., 2015. Tectonic evolution of the southern margin of Laurasia in the Black Sea region. *International Geology Review* 57 (5–8), 1051–1076.
- Okay, A.I., Topuz, G., 2017. Variscan orogeny in the Black Sea region. *International Journal of Earth Sciences* 106 (2), 569–592.
- Okay, A.I., Tüysüz, O., Satır, M., Özkan-Altyner, S., Altyner, D., Sherlock, S., Eren, R.E., 2006. Cretaceous and Triassic subduction-accretion, HP-LT metamorphism and continental growth in the Central Pontides, Turkey. *Geological Society of America Bulletin* 118, 1247–1269.
- Okay, A.I., Satır, M., Shang, C.K., 2008. Ordovician metagranitoid from the Anatolide-Tauride Block, northwest Turkey: geodynamic implications. *Terra Nova* 20 (4), 280–288.
- Okay, A.I., Sunal, G., Tüysüz, O., Sherlock, S., Keskin, M., Kylander-Clark, A.R.C., 2014. Low-pressure–high-temperature metamorphism during extension in a jurassic magmatic arc, Central Pontides, Turkey. *Journal of Metamorphic Geology* 32, 49–69.
- Önen, A.P., 2003. Neotethyan ophiolitic rocks of the Anatolides of NW Turkey and comparison with Tauride ophiolites. *Journal of the Geological Society* 160, 947–962.
- Othman, D.B., White, W.M., Patchett, J., 1989. The geochemistry of marine sediments, island arc magma genesis, and crust-mantle recycling. *Earth and Planetary Science Letters* 94 (1–2), 1–21.
- Oxburgh, E.R., 1972. Flake tectonics and continental collision. *Nature* 239, 202–204.
- Palandjyan, S.A., 1971. The Petrology of Ultrabasites and Gabbroic Rocks of the Sevan Mountain Chain. Izdatelstvo NAS Arm. SSR, 201 p. (in Russian).
- Pallister, S.J., Knight, R.J., 1981. Rare earth element geochemistry of the Semail ophiolite near Ibra, Oman. *Journal of Geophysical Research* 86, 2673–2697.
- Palmer, M.R., Edmond, J.M., 1989. The strontium isotope budget of the modern ocean. *Earth and Planetary Science Letters* 92, 11–26.
- Parlak, O., Delaloye, M., 1999. Precise  $^{40}\text{Ar}/^{39}\text{Ar}$  ages from the metamorphic sole of the Mersin Ophiolite (southern Turkey). *Tectonophysics* 301, 145–158.
- Parlak, O., Çolakoğlu, A., Dönmez, C., Sayak, H., Yıldırım, N., Türk, A., Odabaşı, Y., 2012. Geochemistry and tectonic significance of ophiolites along the Ankara-Erzincan suture zone in northeastern Anatolia. *Geological Society, London, Special Publications* 372, 75–105.
- Pearce, J.A., Harris, N.B., Tindle, A.G., 1984. Trace element discrimination diagrams for the tectonic interpretation of granitic rocks. *Journal of Petrology* 25, 956–983.
- Pessagno, E.A., Ghazi, A.M., Karimina, M., Duncan, R.A., Hassaniapak, A.A., 2005. Tectonostratigraphy of the Khoy complex, northwestern Iran. *Stratigraphy* 2, 49–63.
- Pidgeon, R.T., Bosch, D., Bruguier, O., 1996. Inherited zircon and titanite U-Pb systems in an Archaean syenite from southwestern Australia: implications for U-Pb stability of titanite. *Earth and Planetary Science Letters* 141, 187–198.
- Piegras, D.J., Wasserburg, G.J., 1987. Rare-earth element transport in the western North-Atlantic inferred from Nd isotopic observations. *Geochimica et Cosmochimica Acta* 51, 1257–1271.
- Plank, T., Langmuir, C.H., 1998. The chemical composition of subducting sediment and its consequences for the crust and mantle. *Chemical Geology* 145, 325–394.
- Plunder, A., Agard, P., Chopin, C., Soret, M., Okay, A.I., Whitechurch, H., 2016. Metamorphic sole formation, emplacement and blueschist facies overprint: early subduction dynamics witnessed by western Turkey ophiolites. *Terra Nova* 28 (5), 329–339.
- Rehka, M., Hofmann, A.W., 1997. Recycled ocean crust and sediment in Indian Ocean MORB. *Earth and Planetary Science Letters* 147 (1), 93–106.
- Rezeau, H., Moritz, R., Wotzlaw, J.F., Tayan, R., Melkonyan, R., Ulianov, A., et al., 2016. Temporal and genetic link between incremental pluton assembly and pulsed porphyry Cu-Mo formation in accretionary orogens. *Geology* 44 (8), 627–630.
- Rezeau, H., Moritz, R., Leuthold, J., Hovakimyan, S., Tayan, R., Chiaradia, M., 2017. 30 Myr of cenozoic magmatism along the Tethyan margin during Arabia-Eurasia accretionary orogenesis (Meghri-Ordubad pluton, southernmost lesser Caucasus). *Lithos* 288, 108–124.
- Ribes, C., Kergaravat, C., Crumeyrolle, P., Lopez, M., Bonnel, C., Poisson, A., et al., 2017. Factors controlling stratigraphic pattern and facies distribution of fluvio-lacustrine sedimentation in the Sivas mini-basins, Oligocene (Turkey). *Basin Research* 29 (S1), 596–621.
- Rice, S.P., Robertson, A.H.F., Ustaömer, T., Ýnan, N., Tasly, K., 2009. Late cretaceous–early Eocene tectonic development of the Tethyan suture zone in the Erzincan area, eastern Pontides, Turkey. *Geological Magazine* 146, 567–590.
- Ricou, L.E., Dercourt, J., Geyssant, J., Grand-Jaquet, C., Leprier, C., Biju-Duval, B., 1986. Geological constraints on the alpine evolution of the Mediterranean Tethys. *Tectonophysics* 123, 83–122.
- Roux, M., Bowring, S., Kelemen, P., Gordon, S., Dudás, F., Miller, R., 2012. Rapid crustal accretion and magma assimilation in the Oman-UAE ophiolite: high precision U-Pb zircon geochronology of the gabbroic crust. *Journal of Geophysical Research Solid Earth* 117 (B7).
- Robertson, A.H., Mountakis, D., 2006. Tectonic development of the Eastern Mediterranean region: an introduction. *Geological Society, London, Special Publications* 260, 1–9.
- Robertson, A., Parlak, O., Ustaömer, T., Tasly, K., Ýnan, N., Dumitrica, P., Karaödalan, F., 2013. Subduction, ophiolite genesis and collision history of Tethys adjacent to the Eurasian continental margin: new evidence from the Eastern Pontides, Turkey. *Geodinamica Acta* 26, 230–293.
- Roddick, J.C., Cameron, W.E., Smith, A.G., 1979. Permo-Triassic and Jurassic  $^{40}\text{Ar}/^{39}\text{Ar}$  ages from Greek ophiolites and associated rocks. *Nature* 279, 788–790.
- Rolland, Y., 2017. Caucasus collisional history: review of data from East Anatolia to west Iran. *Gondwana Research* 49, 130–146.
- Rolland, Y., Billo, S., Corsini, M., Sosson, M., Galoyan, G., 2009a. Blueschists of the Amassia-Stepanavan suture zone (Armenia): linking Tethys subduction history from E-Turkey to W-Iran. *International Journal of Earth Sciences* 98, 533–550.
- Rolland, Y., Galoyan, G., Bosch, D., Sosson, M., Corsini, M., Fornari, M., Verati, C., 2009b. Jurassic back-arc and Cretaceous hot-spot series in the Armenian ophiolites – implications for the obduction process. *Lithos* 112, 163–187.
- Rolland, Y., Galoyan, G., Sosson, M., Melkonian, R., Avagyan, A., 2010. The Armenian ophiolite: insights for jurassic back-arc formation, lower Cretaceous hot spot magmatism and upper Cretaceous obduction over the South Armenian block. *Geological Society, London, Special Publications* 340, 353–382.
- Rolland, Y., Sosson, M., Adamia, Sh., Sadradze, N., 2011. Prolonged Variscan to Alpine history of an active Eurasian margin (Georgia, Armenia) revealed by  $^{40}\text{Ar}/^{39}\text{Ar}$  dating. *Gondwana Research* 20, 798–815.
- Rolland, Y., Perincek, D., Kaymakci, N., Sosson, M., Barrier, E., Avagyan, A., 2012. Evidence for 80–75 Ma subduction jump during anatolide-Tauride–Armenian block accretion and 48 Ma Arabia-Eurasia collision in lesser Caucasus–east Anatolia. *Journal of Geodynamics* 56, 76–85.
- Rolland, Y., Hässig, M., Bosch, D., Meijers, M.J.M., et al., 2016. A review of the plate convergence history of the East Anatolia-Transcaucasus region during the Variscan: insights from the Georgian basement and its connection to the Eastern Pontides. *Journal of Geodynamics* 96, 131–145.
- Saccani, E., Dilek, Y., Marroni, M., Pandolfi, L., 2015. Continental margin ophiolites of Neotethys: remnants of ancient Ocean-Continent Transition Zone (OCTZ) lithosphere and their geochemistry, mantle sources and melt evolution patterns. *Episodes* 38 (4), 230–249.
- Sahakyan, L., Bosch, D., Sosson, M., Avagyan, A., Galoyan, G., Rolland, Y., et al., 2017. Geochemistry of the Eocene magmatic rocks from the Lesser Caucasus area

- (Armenia): evidence of a subduction geodynamic environment. Geological Society, London, Special Publications 428, SP428–12.
- Salter, V.J., White, W.M., 1998. Hf isotope constraints on mantle evolution. *Chemical Geology* 145 (3), 447–460.
- Sarifikasioglu, E., Dilek, Y., Sevin, M., 2017. New synthesis of the Izmir-Ankara-Erzincan suture zone and the Ankara mélange in northern Anatolia based on new geochemical and geochronological constraints. Tectonic evolution, collision, and seismicity of Southwest Asia. In: Honor of Manuel Berberian's Forty-Five Years of Research Contributions. Geological Society of America Special Paper, p. 525.
- Scott, D.J., St-Onge, M.R., 1995. Constraints on Pb closure temperature in titanite based on rocks from the Ungava orogen, Canada: implications for U-Pb geochronology and PT path determinations. *Geology* 23 (12), 1123–1126.
- Seccia, A., Montanini, A., Bosch, D., Macera, P., Cluzel, D., 2017. Melt extraction and enrichment processes in the New Caledonia lherzolites: evidence from geochemical and Sr–Nd isotope data. *Lithos* 260, 28–43.
- Şengör, A.M.C., Yılmaz, Y., 1981. Tethyan evolution of Turkey: a plate tectonic approach. *Tectonophysics* 75 (3–4), 181–241.
- Şengör, A.M.C., Altýner, D., Cin, A., Ustaömer, T., Hsü, K.J., 1988. Origin and assembly of the Tethyside orogenic collage at the expense of Gondwana-Land. In: Audley-Charles, M.G., Hallam, A. (Eds.), *Gondwana and Tethys*, vol. 37. Geological Society, London, Special Publications, pp. 119–181.
- Şengün, M., 2006. A critical review of the Anatolian geology: a dialectic to sutures and evolution of the Anatolian Tethys and Neotethys. *Mineral Research Exploration Bulletin* 133, 1–29.
- Shervais, J.W., 1982. Ti-V plots and the petrogenesis of modern and ophiolitic lavas. *Earth and Planetary Science Letters* 59 (1), 101–118.
- Sokolov, S.D., 1977. The Olistostromes and Ophiolitic Nappes of the Lesser Caucasus. Nauka, Moscow (in Russian).
- Sosson, M., Rolland, Y., Danelian, T., Muller, C., Melkonyan, R., Adamia, S., et al., 2010. Subductions, obduction and collision in the Lesser Caucasus (Armenia, Azerbaijan, Georgia), new insights. Geological Society, London, Special Publications 340, 329–352.
- Spray, J.G., Bébian, J., Rex, D.C., Roddick, J.C., 1984. Age constraints on the igneous and metamorphic evolution of magmatism in the Hellenic–Dinaric ophiolites. In: Dixon, J.E., Robertson, A.H.F. (Eds.), *The Geological Evolution of the Eastern Mediterranean*, vol. 17. Geological Society of London, Special Publication, pp. 619–627.
- Stampfli, G.M., Borel, G.D., Cavazza, W., Mosar, J., Ziegler, P.A., 2001. Palaeotectonic and palaeogeographic evolution of the western Tethys and PeriTethyan domain (IGCP Project 369).  *Episodes* 24, 222–228.
- Stocklin, J., 1974. Possible ancient continental margins in Iran. *The Geology of Continental Margins* 873–887.
- Sun, S.S., McDonough, W.F., 1989. Chemical and isotopic systematics of oceanic basalts: implications for mantle composition and processes. In: Saunders, A.D., Norry, M.J. (Eds.), *Magma in Ocean Basins*, vol. 42. Geol. Soc. London, Spec. Publ., pp. 313–345.
- Tachikawa, K., Jeandel, C., Roy-Barman, M., 1999. A new approach to the Nd residence time in the ocean: the role of atmospheric inputs. *Earth and Planetary Science Letters* 170, 433–446.
- Taylor, S.R., McLennan, S.M., 1985. *The Continental Crust: its Composition and Evolution*. Blackwell, 312 p.
- Tekin, U.K., Ural, M., Göncüoğlu, M.C., Arslan, M., Kürüm, S., 2015. Upper Cretaceous Radiolarian ages from an arc–back-arc within the Yüksekoval Complex in the southern Neotethys mélange, SE Turkey.  *Comptes Rendus Palevol* 14 (2), 73–84.
- Thirlwall, M.F., 1997. Pb isotopic and elemental evidence for OIB derivation from young HIMU mantle. *Chemical Geology* 139 (1), 51–74.
- Topuz, G., Çelik, Ö.F., Şengör, A.M.C., Altýntap, Y.E., Zack, T., Rolland, Y., Barth, M., 2013a. Jurassic ophiolite formation and emplacement as backstop to a subduction-accretion complex in Northeast Turkey, the Refahiye ophiolite, and relation to the Balkan ophiolites. *American Journal of Science* 313, 1054–1087.
- Topuz, G., Göcmengil, G., Rolland, Y., Çelik, Ö.F., Zack, T., Schmitt, A.K., 2013b. Jurassic accretionary complex and ophiolite from northeast Turkey: no evidence for the Cimmerian continental ribbon. *Geology* 41, 255–258.
- Topuz, G., Candan, O., Zack, T., Yilmaz, A., 2017. East Anatolian plateau constructed over a continental basement: No evidence for the East Anatolian accretionary complex. *Geology* 45 (9), 791–794.
- Ural, M., Arslan, M., Göncüoğlu, M.C., Tekin, K.U., Kürüm, S., 2015. Late Cretaceous arc and back-arc formation within the Southern Neotethys: whole-rock, trace element and Sr-Nd-Pb isotopic data from basaltic rocks of the Yüksekoval Complex (Malatya-Elazığ, SE Turkey). *Ophioliti* 40 (1).
- Ustaömer, T., Robertson, A.H.F., 2010. Late palaeozoic–early cenozoic tectonic development of the eastern Pontides (Artvin area), Turkey: stages of closure of Tethys along the southern margin of Eurasia. In: Sosson, M., Kaymakçy, N., Bergerat, F., Starostenko, V. (Eds.), *Sedimentary Basin Tectonics from the Black Sea and Caucasus to the Arabian Platform*, vol. 340. Geological Society, London, Special Publications, pp. 281–327.
- Ustaömer, T., Robertson, A.H.F., Ustaömer, P.A., Gerdes, A., Peytcheva, I., 2013. Constraints on Variscan and Cimmerian magmatism and metamorphism in the Pontides (Yusufeli-Artvin area), NE Turkey from U-Pb dating and granite geochemistry. Geological Society, London, Special Publications 372, 49–74.
- Vanderhaeghe, O., 2012. The thermal–mechanical evolution of crustal orogenic belts at convergent plate boundaries: a reappraisal of the orogenic cycle. *Journal of Geodynamics* 56, 124–145.
- Vannucchi, P., Remitti, F., Bettelli, G., 2008. Geologic record of fluid flow and seismogenesis along an erosive subducting plate boundary. *Nature* 451, 699–703.
- Vaughan, A.P., Scarrow, J.H., 2003. K-rich mantle metasomatism control of localization and initiation of lithospheric strike-slip faulting. *Terra Nova* 15, 163–169.
- Vaughan, A.P.M., Scarrow, J.H., 2003. Ophiolite obduction pulses as a proxy indicator of superplume events? *Earth Planet. Science Letters* 213, 407–416.
- Vincent, S.J., Saintot, A., Mosar, J., Okay, A.I., Nikishin, A.M., 2017. Comment on 'Relict basin closure and crustal shortening budgets during continental collision: an example from Caucasus sediment provenance' by Cowgill et al. [2016]. *Tectonics* 37. <https://doi.org/10.1002/2017TC004515>.
- Warren, J.M., 2016. Global variations in abyssal peridotite compositions. *Lithos* 248, 193–219.
- Whitechurch, H., Omrani, J., Agard, P., Humbert, F., Montigny, R., Jolivet, L., 2013. Evidence for Paleocene–Eocene evolution of the foot of the Eurasian margin (Kermanshah ophiolite, SW Iran) from back-arc to arc: implications for regional geodynamics and obduction. *Lithos* 182, 11–32.
- Whitney, D.L., Evans, B.W., 2010. Abbreviations for names of rock-forming minerals. *American Mineralogist* 95, 185–187.
- Yalınız, K.M., Floyd, P.A., Göncüoğlu, M.C., 2000. Geochemistry of volcanic rocks from the Çıçekdağ, ophiolite, central Anatolia, Turkey, and their inferred tectonic setting within the northern branch of the Neotethyan ocean. Geological Society, London, Special Publications 173 (1), 203–218.
- Yamato, P., Agard, P., Burov, E., Le Pourhiet, L., Jolivet, L., Tibéri, C., 2007. Burial and exhumation in a subduction wedge: mutual constraints from thermo-mechanical modeling and natural P–T–t data (Sch. Lustrés, W. Alps). *Journal of Geophysical Research* 112, B07410.
- Yilmaz, Y., Tüysüz, O., Yigitbas, E., Can Genç, S., Şengör, A.M.C., 1997. Geology and tectonic evolution of the Pontides. In: Robinson, A.G. (Ed.), *Regional and Petroleum Geology of the Black Sea and Surrounding Region: American Association of Petroleum*, vol. 68. Geologists Memoir, pp. 183–226.
- Yilmaz, A., Yilmaz, H., Kaya, C., Boztug, D., 2010. The nature of the crustal structure of the Eastern Anatolian Plateau, Turkey. *Geodinamica Acta* 23 (4), 167–183.
- Yilmaz, A., Yilmaz, H., 2013. Ophiolites and ophiolitic mélanges of Turkey: a review. *Geological Bulletin of Turkey* 56, 119–172.
- Zakariadze, G.S., Dilek, Y., Bogdanovsky, O.G., Karpenko, S.F., Vishnevskaya, V.S., Solov'eva, N.V., 2005. Age Limits of the Lesser Caucasus Paleo-Oceanic Allochthon. Active Tectonics of the Aegean Region, 15–18 June 2005. Kadir Has University, Istanbul, Turkey, p. 229.
- Zindler, A., Hart, S.R., 1986. Chemical geodynamics. *Annual Review of Earth and Planetary Sciences* 14, 493–571.